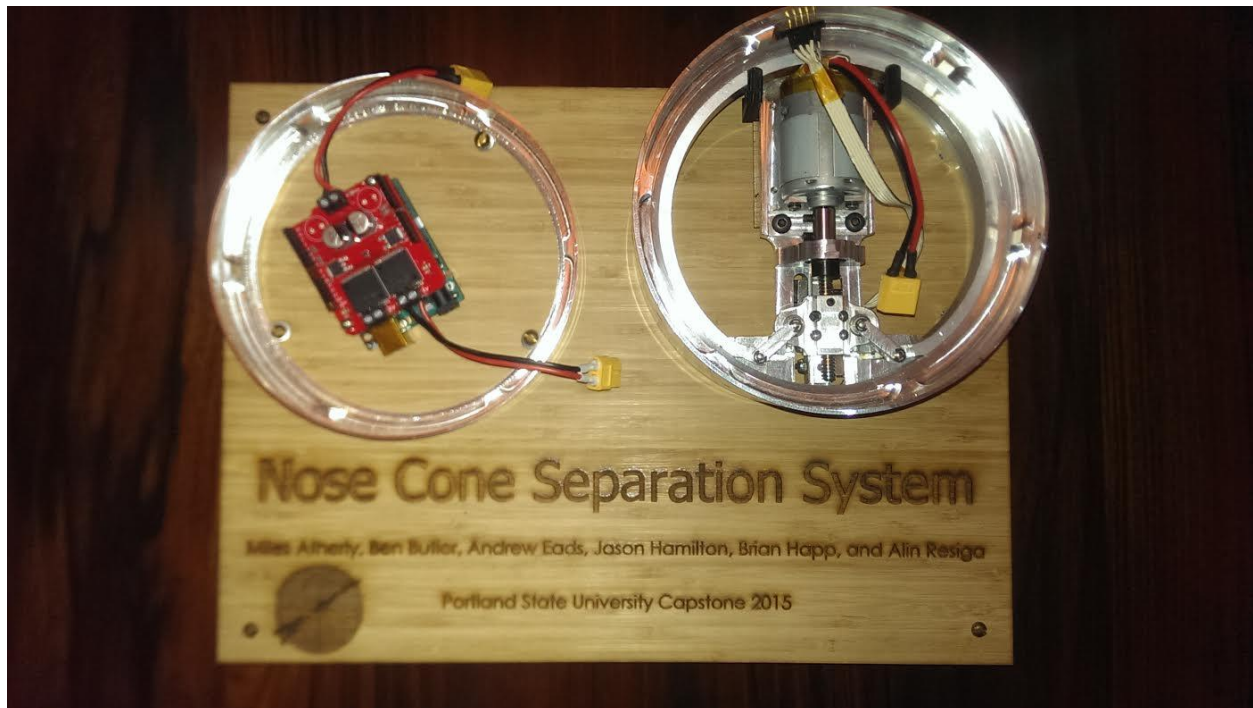


Nose Cone Separation Ring for LV3 High Altitude Sounding Rocket

Miles Atherly, Benjamin Butler, Andrew Eads, Jason Hamilton, Brian
Happ, Alin Resiga

Advisor: Dr. David Turcic



Executive Summary

An electro-mechanical Nosecone Separation Ring (NSR) system was developed for Portland State Aerospace Society (PSAS). The electro-mechanical NSR will replace PSAS' current NSR mechanism, which uses a bonding agent and gunpowder charges. The new NSR will address several shortcomings exhibited by the current separation device.

The electro-mechanical NSR uses a DC motor, linear guide rail, ¼-16 ACME power screw, and relative motion arms, guide pins, and rails to actuate an aluminum v-shaped clamping band over two angled surfaces. A wave spring, which provides a kickoff force upon separation, is inlaid into a groove in the larger (male) coupling ring. Currently, the prototype NSR is controlled by pulse width modulation (PWM) via an Arduino Uno R3. Two limit switches control fore and aft travel of the sled during actuation, and cut the power to the motor. In its current design state, the NSR is capable of deploying in less than 63 milliseconds.

Physical testing, finite element analysis, and mathematical models were used to verify reliability of critical components in the new NSR system. The most critical component, which also bears the highest stress during actuation, is the aluminum clamping band. The design of the band was optimized so that it has a minimum factor of safety of 1.67 throughout the actuation.

Table of Contents	Page
1.0 Introduction	X
2.0 Mission Statement	X
3.0 Main Design requirements	X
4.0 Top-Level Design Decision	

5.0	Final Design	X
6.0	Evaluations of Components	
6.1.	V-Band Sizing and Analysis	
6.2.	Clamped Surface Analysis	
6.3.	Motor Sizing	X
7.0	Evaluations as Related to PDS	X
8.0	Conclusions and Recommendations	
	Acknowledgements	
	Bibliography	
	Appendix A: Detailed Design	
	Appendix B: DFMEA on V-band	
	Appendix C: Potential Yielding at Critical Point	
	Appendix D: Bill of Materials	
	Appendix E: Analysis Based Design Decisions	
	Appendix F Assembly Instructions	
	Appendix G: Drawings	

1.0 Introduction

Portland State Aerospace Society (PSAS) was founded in 1997 with the goal of putting a nano-satellite into orbit. PSAS is in the process of building their third sounding rocket, and is redesigning several aspects of this rocket, including the nose cone separation mechanism. Currently, the nose cone is adhered to the main body of the rocket with epoxy. A small amount of gunpowder is deposited throughout a cavity between the nose cone and body. At apogee, the gunpowder is ignited via electric matches, breaking the bond of the epoxy. An internal plunger assembly then pushes the nose

cone off the rocket, deploying the parachute. This separation method is not easily testable, but does allow the rocket to be recovered and reused. PSAS would like an easily testable, reliable, and more efficient way of releasing the nose cone and deploying the parachute. Ideally, the new parachute deployment mechanism would be easy to reset and not use any consumables, such as gunpowder.

Four main separation mechanisms were used to draw ideas from. A Marmon clamp, a Lightband™, gas actuated pins, and an electromagnetic lock. An electro-mechanical device similar to the Marmon Clamp, and the V-Band, was chosen for its simplicity and reliability. The design relies on the expansion and contraction of an angled band to clamp the upper and lower rings of the rocket together. This device increases the diameter of the clamping band using a power screw driven by a motor. Since the power screw is self-locking, the two rings stay clamped without additional power. The motor reverses the direction of the power screw, and the rings become unclamped in under 63 milliseconds. The electro-mechanical NSR meets all of the design requirements; it is easily resettable, easily testable, and will withstand the forces it will experience in flight.

2.0 Mission Statement

The mission of the NSR team was to design and prototype a device that will facilitate the separation of the nose cone from the main body of the rocket. The device needs to be easily testable, resettable, and have a failure rate of less than one percent. The device must not impede the parachute deployment, and needs to be completed by June, 5, 2015 with a budget of \$3,000.

3.0 Main Design Requirements

The current NSR cannot be tested without firing the gunpowder charges which makes it difficult to predict if the separation ring has been prepared correctly before launch. The

epoxy used to bind the nose cone to the body takes several hours to cure, so if any problems are detected before launch they cannot be corrected on the same day. PSAS would like to replace their existing NSR with an electro-mechanical device that can be tested, easily reset, and have a verifiable failure rate of less than one percent. This would allow them to check the NSR mechanism on launch days. If the device were to fail, it needs to fail in the closed position (i.e.-the nose cone remains attached to the airframe in the event of system failure). This is significantly safer than failing in the open position (i.e- the nose cone is detached from the airframe in the event of system failure)

The NSR should use no more than 5W of standby power and no more than 50W of power to actuate from the main battery. The device also needs to be operable in a vacuum, and withstand a tensile force of 250lb PSAS requested, but did not require that the design of the NSR be modular and scalable so that it can be adapted for stage release applications and for larger diameter rockets in the future.

4.0 Top-Level Design Decision

The three main concepts that were pursued were an electro-mechanical device driven by a stepper motor, a compressed gas powered 4- pin actuator, and an electromagnetic lock. The gas powered 4-pin actuator was discarded due to difficulties designing it to fail in a closed position. An electromagnetic lock design was quickly discarded because the magnets could be damaged upon touchdown impact. Ultimately, the decision was made to use a clamp similar to the V-band and Marmon clamp driven by a DC stepper motor. Later, the stepper motor was replaced with a brushed DC motor as it is easier to manipulate, can be over-driven, and will satisfy the speed and power requirements of the proposed design.

From the external and internal search, a concept scoring matrix was used to decide between alternative ideas. The results are summarized in Table 1. The V-band has the highest score, and was used as a starting point for the NSR design.

Table 1. Concept Scoring Matrix: Larger numbers correspond to more desirable qualities

	V-band	Lightband™	Gas Actuated Pins	Electromagnetic
Speed	3	3	4	5
Manufacturing Complexity	4	3	3	2
Power System	4	4	2	2
Binding Risk	4	3	2	4
Totals	15	13	11	13

The primary reason for designing a mechanism similar to the V-band instead of something more similar to the Lightband™ was due to manufacturing complexity. The Lightband™ uses a series of right angle clamps to hold down the upper ring. These clamps are fixed to the bottom with a shear pin. Creating this design would involve sourcing or machining eight to ten of these right angle clamps, and designing a way to fixture them to the lower ring. Having all of these components might also increase the risk of loading failure. For example, the shear pins could break or the top part of the right angle clamp could shear off. The decision was also made to clamp from the inside instead of the more traditional style of clamping from the outside to keep the rocket as aerodynamic as possible. Figure 1 is a cut-away model of the design where some of the design aspects are seen..

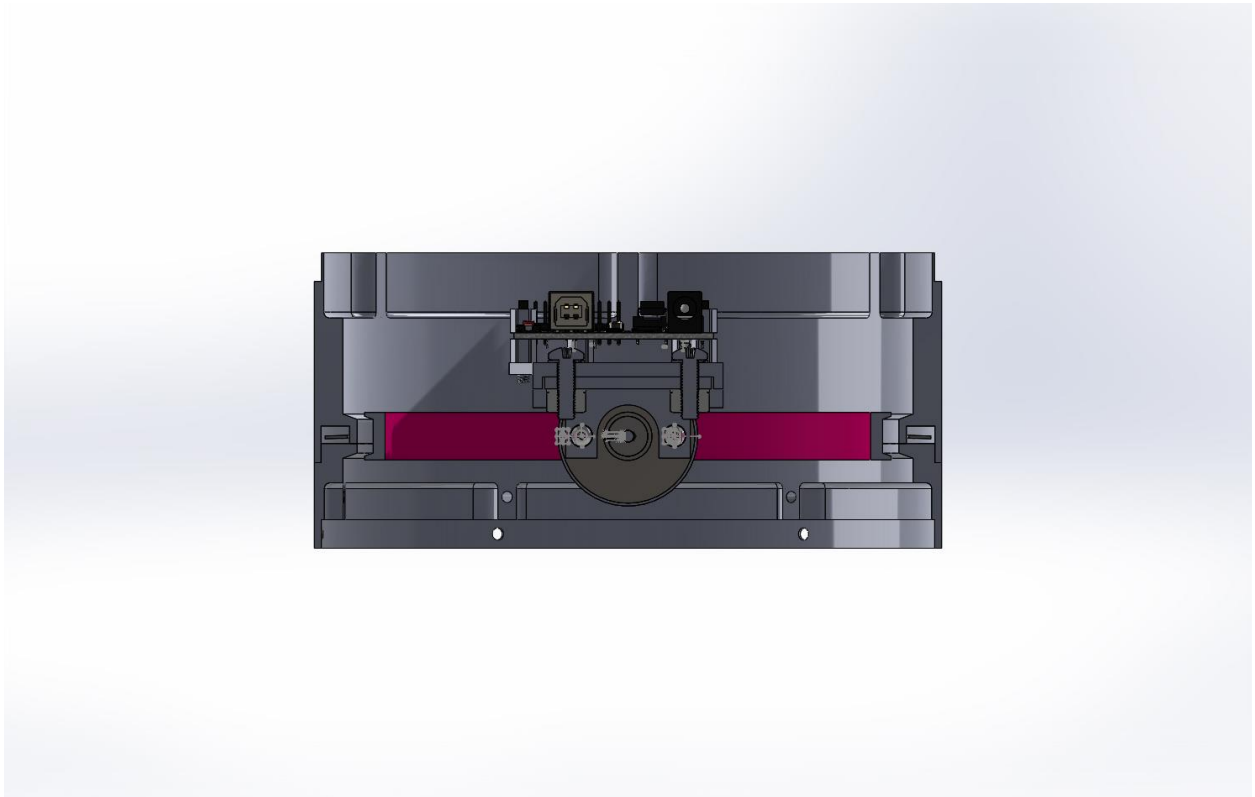


Figure 1- An isometric cut-away view of the initial design proposal. The design incorporates aspects of both the Marmon Clamping System and the Lightband™ separation device.

The NSR design utilizes an internal inverted marmon clamp. The actuation of the inverted marmon clamp works similarly to the Lightband™ in that the actuation is started by translating rotational motion from a DC motor into linear motion. The similarities between the two devices end there, as the NSR's clamping mechanism significantly differs from that of the Lightband™.

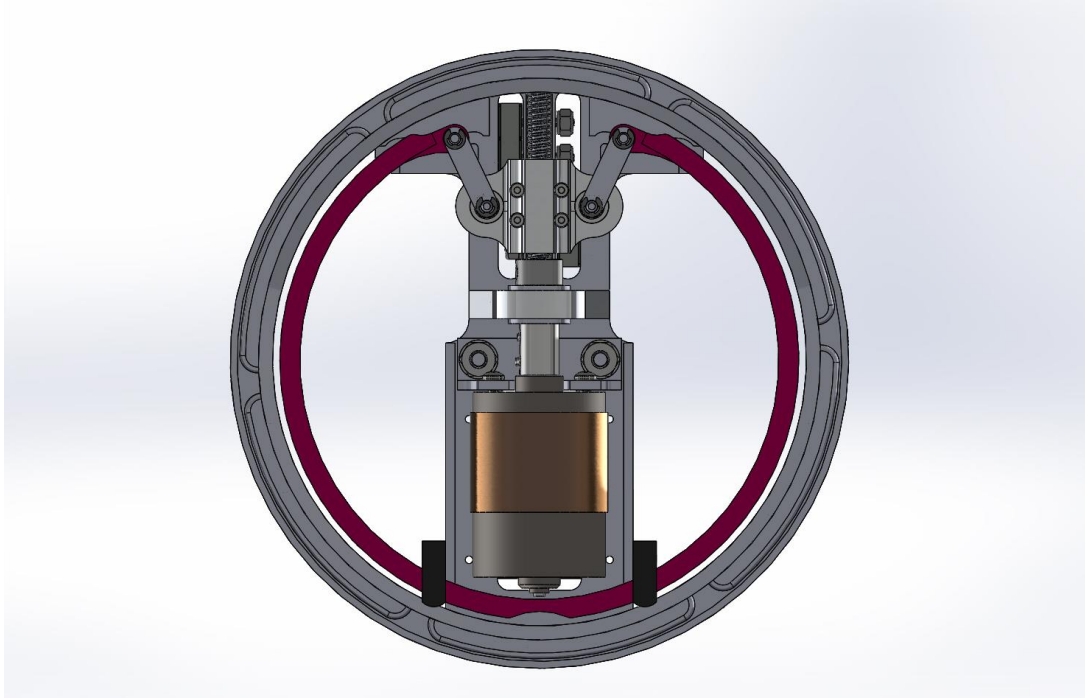


Figure 2- Top down view of the separation mechanism.

5.0 Final Design

The purpose of the mechanism is to provide a clamping force from the V-band simultaneously to the upper and lower rings to hold the nose cone to the rocket during flight. Then, at the desired point in flight, release the nose cone and deploy the parachutes by rapidly contracting the V-band. The nose cone is attached to the upper coupling ring (female) and the main body of the rocket is attached to the lower coupling ring (male).

The NSR mechanism is powered independently by an 11.1 V Lithium Polymer battery. Actuation is started by sending a signal from the flight computer to the control

board which powers the motor and drives the V-band to either an open or closed position. The power screw rides on and is supported by the journal and a pair of needle thrust bearings. The sled rides back and forth along the power screw, which provides two important functions; direct horizontal motion for sliding the V-band forward or back to either clamp or release the nose cone, and to actuate the relative motion arms to open or contract the V-band.

During the clamping or unclamping sequence, the sled will contact one of two limit switches mounted under the device. The limit switches signal the control board to stop the motor and end the actuation sequence. The actuator is attached to the upper, larger, coupling which will be attached to the nose cone. Upon deployment, the actuator will separate from the rocket body with the nose cone, allowing plenty of space for the drogue and main parachutes to deploy through. Figure 3 is a bottom up view of the complete NSR mechanism. Not pictured are the arduino and the battery.

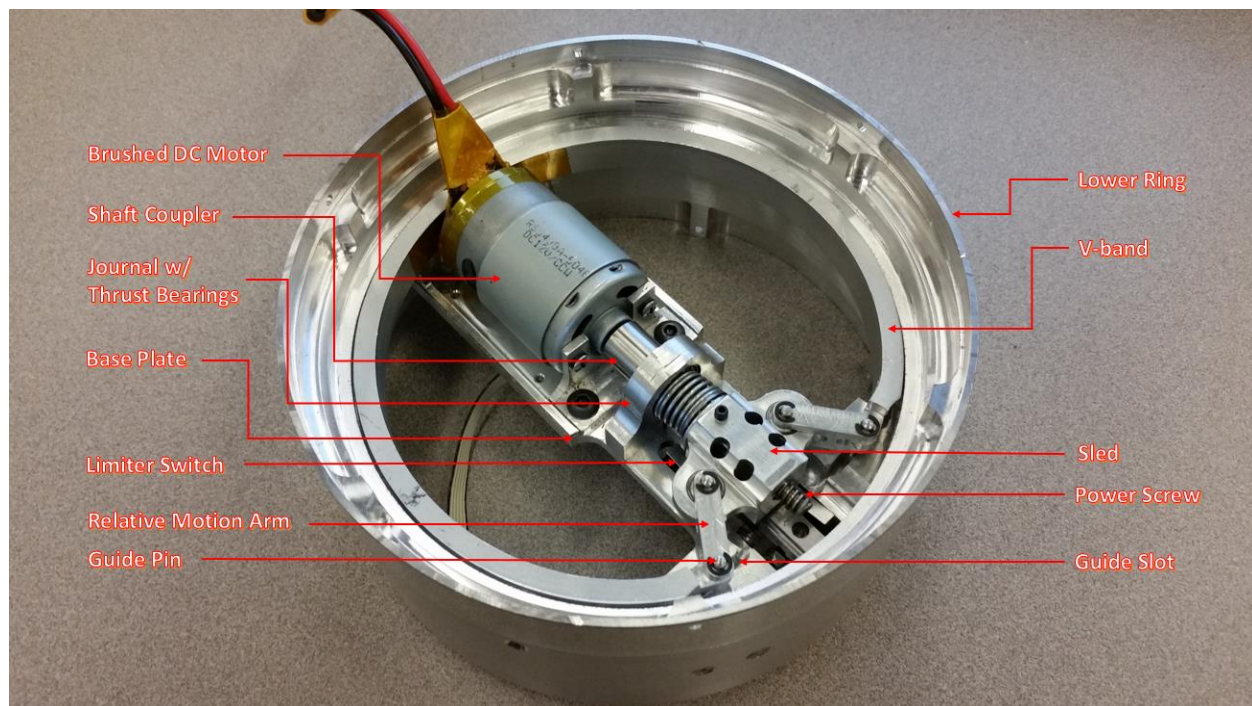


Figure 3: A bottom up view of the complete NSR assembly.

The NSR components are a combination of in-house custom manufactured components and prefabricated outsourced components. The in-house manufactured components

include both coupling rings, V-band, journal, shaft coupler, sled, motor mount, dowel pins, male indexing tabs, and actuator arms. The outsourced parts include the power screw, thrust bearings, 7mm guide rail, 7mm carriage, motor, control board, LiPo battery, wave spring, and all fasteners.

6.0__Evaluation of Components

After the final design concept was approved, three major design points of the NSR were evaluated. The three design points are the V-band, the clamped surface area of the coupling rings, and the power requirements of the system.

6.1 V-Band Sizing and Analysis

A mathematical model constructed using Castigliano's theorem, shown in Appendix E, shows that the force required to displace the tabs of the band depends heavily on the radius of curvature and the cross-sectional area of the band. The force required to displace the band will be reduced by increasing the radius of curvature of the neutral axis, or by decreasing the cross-sectional area of the band. The original V-band design required a load of 10 lbf per side (20 lbf total) to achieve a net displacement of 0.8 in.

To determine the stress present in the displaced state of the V-band, an FEA model of the band was built and subjected to a similar load. Meshing properties of the FEA model were adjusted until the force and displacement parameters of the FEA model resembled the force and displacement parameters for the mathematical model. Additionally, a physical experiment was performed in order to validate the results of both the FEA and the mathematical model, shown in Appendix C. Results from the physical experiment matched results from the FEA model and the mathematical model closely, and the FEA model was deemed as a viable design tool for optimizing V-band parameters.

FEA analysis of the original V-band exhibited a maximum stress value of 36.98 kpsi located on the back side of the band on the lip of the clamping surface illustrated in Figure 4. Since the yield strength of 6061-T6 aluminum is 40 kpsi, the original V-band design had a factor of safety of 1.08 in its deployed state. A design revision of the V-band was done in order to increase the factor of safety of the band in the deployed state as well as decrease the force required for displacement. FEA was used as the primary design tool in this process.

The cross-sectional area of the V-band was thinned out significantly by removing material from the web and the lips of the clamping surface. The center of the V-channel was held constant in order to shift the radial distance of the neutral axis outwards. Thinning the web and removing material from the lips of the clamping surface reduced the force required to displace the band from 20 lbf to 6.6 lbf, but did not significantly reduce the maximum observed stress value. 1.5 in diameter relief cut was added to the back wall of the V-band where the maximum stress was observed. The addition of the relief cut reduced the observed stress to 23.92 kpsi and increased the factor of safety to 1.67. The completely revised V-band is seen in Fig. 5 and shows the maximum stress concentration location, and magnitude relative to yield strength of the material.

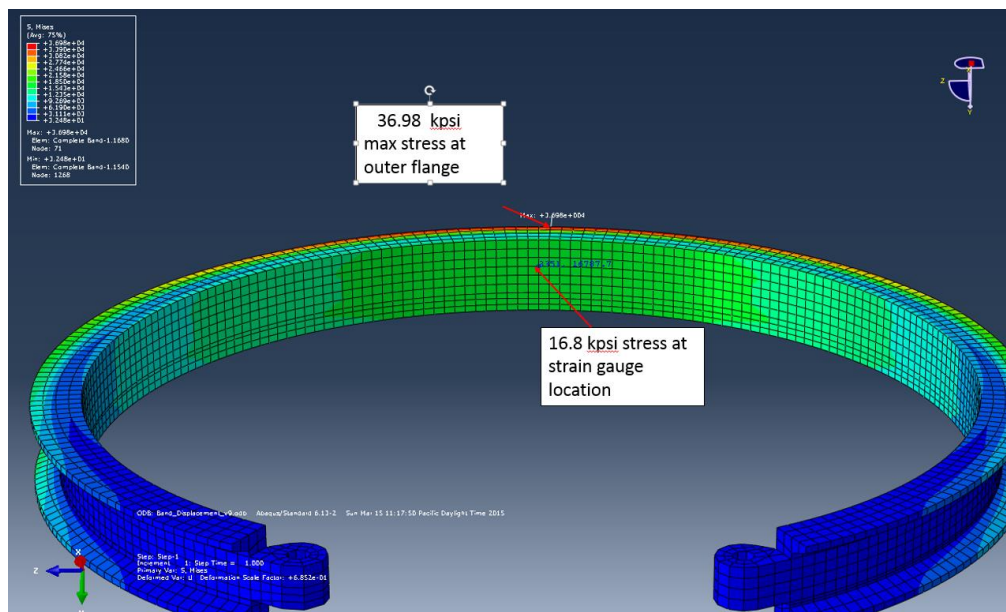


Figure 4: FEA analysis of the location and magnitude of maximum stress concentration.

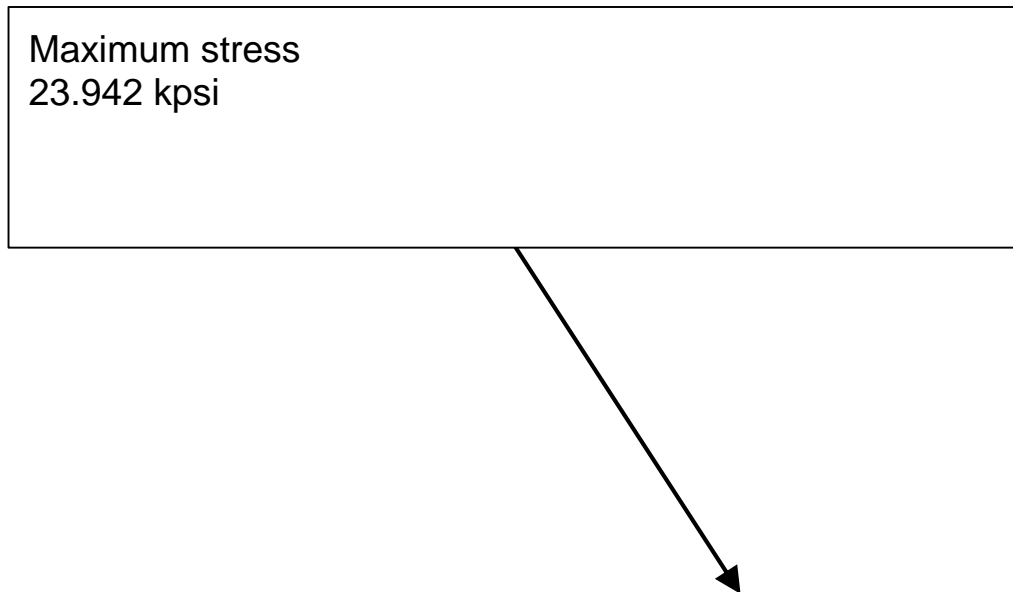


Figure 5: Maximum stress relative to material yielding with smaller webbing and a relief cut.

6.2 Clamped Surface Analysis

Figure 6 shows the cross sectional area that the V-band clamps to inside of the coupling rings. The designed cross sectional area was analyzed using an axial load of 250 lbf in order to determine if the clamped surfaces will yield. The minimum theoretical cross sectional area requirement was calculated to be $5.873 * 10^{-3} in^2$. Figure 6 shows the smallest designed cross sectional area of the clamped surface of $0.0128 in^2$ which will not yield at the theoretical axial load and is ideal as the large cross sectional area adds robustness. For the complete analysis of these design dimensions see Appendix E.

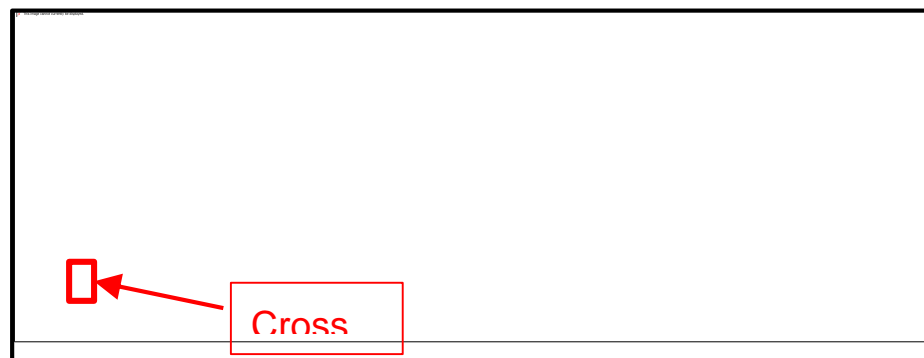


Figure 6: Smallest cross sectional clamping area analyzed for yielding

6.3 Motor Sizing

To accurately size the motor, a torque test on the power screw was performed. To determine the amount of radial deflection the power screw will experience under specific torque loads, and to develop a method to characterize a torque curve for the power screw, a strain analysis was performed on a $\frac{1}{4}$ " steel rod similar in size and material to that of the power screw. The $\frac{1}{4}$ " rod stock seen in Figure 7 with the attached strain gauge was used in lieu of the power screw due to size and shape constraints for applying the available strain gauge to the power screw. The validated torque testing method was then going to be applied to the power screw to determine the maximum torque needed to actuate the V-band. However, the strain gauge method was not used due to difficulties in applying a strain gauge to the turned down $\frac{1}{8}$ " round end of the power screw. The maximum torque required to actuate the V-band was determined to be approximately 3 in-lb. The maximum torque was found by measuring different loads applied to the end of a radial arm which was attached to the power screw in the prototyped model. The load required during the last $\frac{1}{8}$ th turn of the power screw was taken to be the maximum required torque. The maximum determined torque value was multiplied by safety factor of 2 to ensure the selected motor had enough capacity to actuate the V-band within the time limit outlined in the PDS.

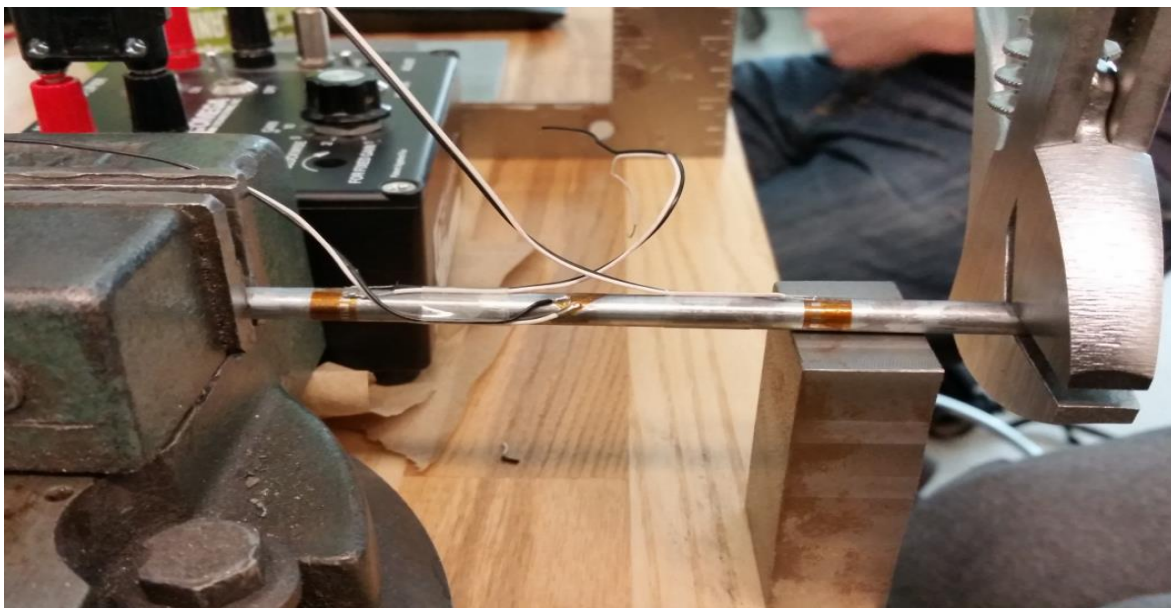


Figure 7: Torque testing on the $\frac{1}{4}$ " rod stock used to validate the torque testing method.

7.0 Evaluations as Related to PDS

The main requirement from PSAS is that the system can be easily reset and quickly tested. The design meets this requirement, and can be actuated and reset several times per minute. The device has an actuation time of 63 milliseconds.

By designing the NSR such that the motor and baseplate assembly are attached to the nosecone, two requirements were met. The parachute can deploy without interference from the device, and there is now room to attach an independent battery. The device requires no power from the main rocket battery, satisfying the power requirements outlined in the PDS.

Using FEA, both loading requirements were verified. See Appendix C for the results. The inside band can withstand the 250lb tensile force with a factor of safety of 30.

As seen in Appendix C, the stress on the V-band is 24 ksi at full actuation. According to Equation 1, the V-band can be fully actuated and brought to rest 44,000 times before being affected by fatigue.

$$N = [2,100,000/(S - 14,000)]^2 \quad (1)^{[9]}$$

Where N is the number of cycles until failure and S is the stress on the part (24 ksi).

The budget for this project was \$3,000. Because most of the machining was done in-house, the final product was made at a fraction of the total budget. The final cost of production was \$1,300.

8.0 Conclusion and Recommendations

An alternative NSR device that does not use consumables, such as epoxy and gunpowder, was developed by the June 5th deadline for a total cost of \$1,300. The system utilizes a unique internal V-band design to apply a clamping force to two customized coupling rings that will be mounted on the LV3 rocket. The new NSR is robust in design. FEA shows that the NSR will be able to sustain tensile loadings of up to 250 lbf with a factor of safety of 30. Fatigue analysis on the V-band shows that it will sustain 44,000 cycles of actuation before failure. The actuation time of the NSR is 63 milliseconds (conservatively), so the device can be tested and reset several times a minute. The system is equipped with its own power source and will not draw more than a nominal amount of power from the main rocket battery. The system is designed to fail in the closed position as requested.

Designing the electro-mechanical NSR presented several unique challenges. The size of the LV3 rocket modules limited the type of actuators that could be used. Designing a clamping system that utilizes bending in key components is unorthodox in nature. The power requirements of the system were such that a custom drive train had to be designed and machined.

A prototype electrical system utilizing an Arduino Uno R3 and a 30 Amp H-Bridge was developed to test the new NSR system. Controlling the system for position and speed has proven to be difficult due to the extremely fast wind up of the motor and the small linear displacement of the actuator. The stall current of the motor is 85 Amps and the no load speed of the motor is 19300 RPM. The use of the 30 Amp H-Bridge limits the motor from operating over its full torque range. The lack of low end power due to the 30 A current ceiling sometimes causes the system to become bound in the forward position. Additionally, the sampling rate of the Arduino Uno is limited to 9600 samples per second. When the NSR is actuating, the motor spins up so fast that the system has a tendency to overshoot the fore and aft limit switches before the power to the motor is braked to the ground pin of the Arduino. This makes the system very difficult to precisely control. The system would benefit from using a faster control board that is not

limited to an amperage below the motors stall current. Additionally the NSR system would benefit from a second type of feedback other than limit switches to avoid binding in the forward or reverse position. A pressure sensor, force transducer, proximity switch, or a more advanced position detection system could be implemented to improve the performance and reliability of the device.

Acknowledgements

The Nosecone Separation Ring group would like to give special acknowledgement to Jeffrey Hickman, Dr. Turcic, Mike Chuning, Andrew Greenberg, Nathan Bergey, Gavin Gallino, Sam Stewart, and all the members of PSAS for their support in this project.

Bibliography

[1] Budynas, Richard G, J K. Nisbett, and Joseph E. Shigley. *Shigley's Mechanical Engineering Design*. New York: McGraw-Hill, 2011. Print.

[2] Dailey, J., 2014. *AFRL Technology Demonstrated on NASA Moon Mission*. [Online] Available at: <http://www.wpafb.af.mil/news/story.asp?id=123418650> [Accessed 8 January 2015].

[3] Dirgo, B., 2013. *Orbital Sciences Corporation Payload Separation System*. [Online] Available at: http://www.cefns.nau.edu/capstone/projects/ME/2014/OrbitalPayloadSeparationSystem/images/carosel_images/4_new.png [Accessed 25 November 2014].

[4] Lazansky, C., 2012. *Refinement of a Low-Shock Separation System*, s.l.: s.n.

[5] NASA, 1970. *Flight Separation Mechanism*, s.l.: s.n.

[6] NASA, n.d. *Marman Clamp System Design Guidelines*, s.l.: s.n.

[7] NEA Electronics Inc., n.d. *Ensign-Bickford Aerospace & Defense*. [Online] Available at: <http://www.eba-d.com/assets/product-sheets-nea/V-Band-Product-Sheet.pdf> [Accessed 8 January 2014].

[8] Sierra Nevada Corporation, n.d. *Qwksep Payload Separation System*. [Online]

Available at:
<http://www.spacedev.com/pdfs/Qwksep%20Payload%20Separation%20System.pdf>
[Accessed 8 January 2015].

[9] Yahr, G. T., 1993. *FATIGUE DESIGN CURVES FOR 6061-T6 ALUMINUM*, Oak Ridge, Tennessee: Oak Ridge National Laboratory.

Appendix A: Detailed Design

The LV3 launch vehicle is composed several modular sections that have an inner diameter of 6 inches and an outer diameter of 6.6 inches. The inner diameter of the modular sections was a major design constraint and was used as the starting point for the NSR design. Castigliano's theorem shows that for a curved beam, the force required to deflect the beam a set distance is dependant on the radius of curvature of the neutral axis of the beam and the cross-sectional area of the beam. Castigliano's theorem was initially used to design the V-band such that the force required to actuate the band within the 6 inch diameter modules would be at a minimum. The clamping surfaces onto which the V-band mated were fixed at 5.7 inches in diameter. A 20 degree angular clamping surface was decided upon, because the angled surface helps guide components into proper placement during mating. The height of the V-band was fixed at 0.5 inches. Single part FEA of the V-band and the clamping surfaces showed that all surfaces could sustain t a 250 lbf tensile load with a factor of safety of 30. FEA was later used to optimize sizing parameters of both the V-band and the coupling ring clamping surfaces.



Figure 1A- Final V-band design.

Actuation of the V-band requires that a pair of equal and opposite forces be applied to the two tabs of the V-band. In order to accomplish this, a linear actuator needed to be designed. FEA, Castigliano's theorem, and real world experimentation showed that a minimum force of 8 lbf per tab was needed to actuate the band. The force requirement combined with the space constraints of the LV3 modules immediately disqualified many traditional prefabricated linear actuators. In order to satisfy the power requirements of the V-band, a high powered brushed DC motor and custom linear actuation mechanism were needed.

A power screw was selected as the preferred method of translating rotational motion to linear motion. In order to keep the torque on the power screw low, a small diameter (0.25 inch) screw was selected. A 7mm precision guide rail and carriage was selected to provide a linear motion constraint to the actuation system. The guide rail is made out of hardened steel and has a dynamic load capacity of 300 lbf. A sled and arm assembly which interfaced with both the carriage and the V-band tabs was designed to transmit the force from the DC motor to the V-band. During actuation, the arms of the sled are allowed to rotate. The sled was fitted with $\frac{1}{8}$ " ID x $\frac{3}{8}$ " OD x $\frac{5}{32}$ " height ball bearings which limit the friction incurred in the arms during actuation.

In order to mate evenly around the entire clamping surface, the center of the V-band must be held constant while the diameter of the band increases. This was accomplished by designing a set of relative motion channels which constrain the motion of the V-band tabs (and sled arms) to a set path. The principles of rigid body kinematics were used to describe the path the arms were required to follow in both rotation and translation.

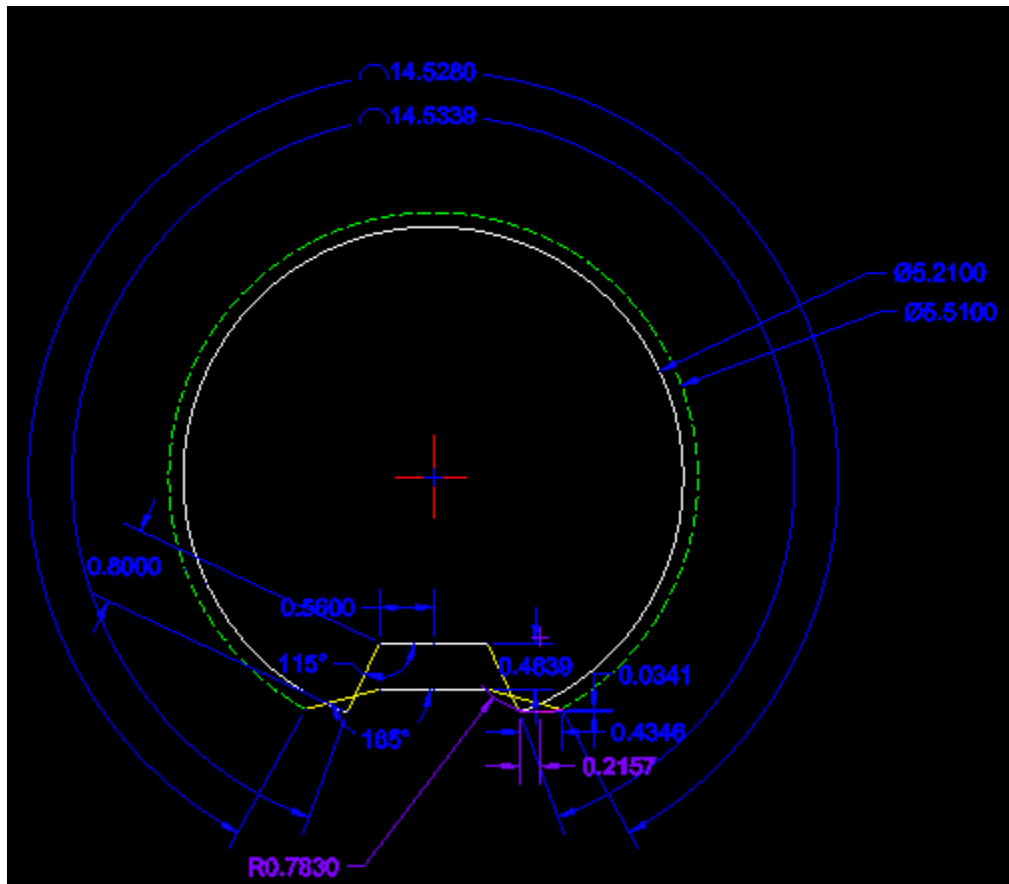


Figure 2A- A graphical representation of the V-band in its “open” and “closed” state. The initial and final angle of the relative motion arms (yellow), and sled (white) are shown. Additionally, the V-band perimeter is shown (solid white, dotted green).

A theoretical torque curve for the entire system was modeled using the required actuation force, sled dimensions, rail dimensions, and power screw dimensions. The model predicted that 6 lbf-in of torque was needed to actuate the power screw. The net linear distance traveled by the sled to accommodate full actuation was found to be 0.4636 inches. This distance corresponds to just over 4 complete rotations of the $\frac{1}{4}$ -16 ACME power screw. A motor that was capable of delivering the determined torque requirements as well as the goal actuation time of 0.1s was selected. The dimensions of the selected motor allowed for direct drive of the device.

A base plate was designed to incorporate all of the above mentioned elements as well as two slots for limit switches. The base plate bridges the 6 inch diameter of the coupling rings for added strength and stability. Single part FEA of the baseplate

showed that it could sustain a 250 lbf concentrated load applied to the part center. The base plate design also includes a 1.5" x 1.5" pattern of 4-40 tapped mounting holes onto which a control board or control board adapter can be mounted. The base plate is held in place with seven 4-40 tapered machine screws which interface with the coupling rings. A modular stem was designed to mount to the bottom of the baseplate. The modular stem adds additional structural stability as well as providing a surface onto which limit switches and other feedback mechanisms can be mounted.

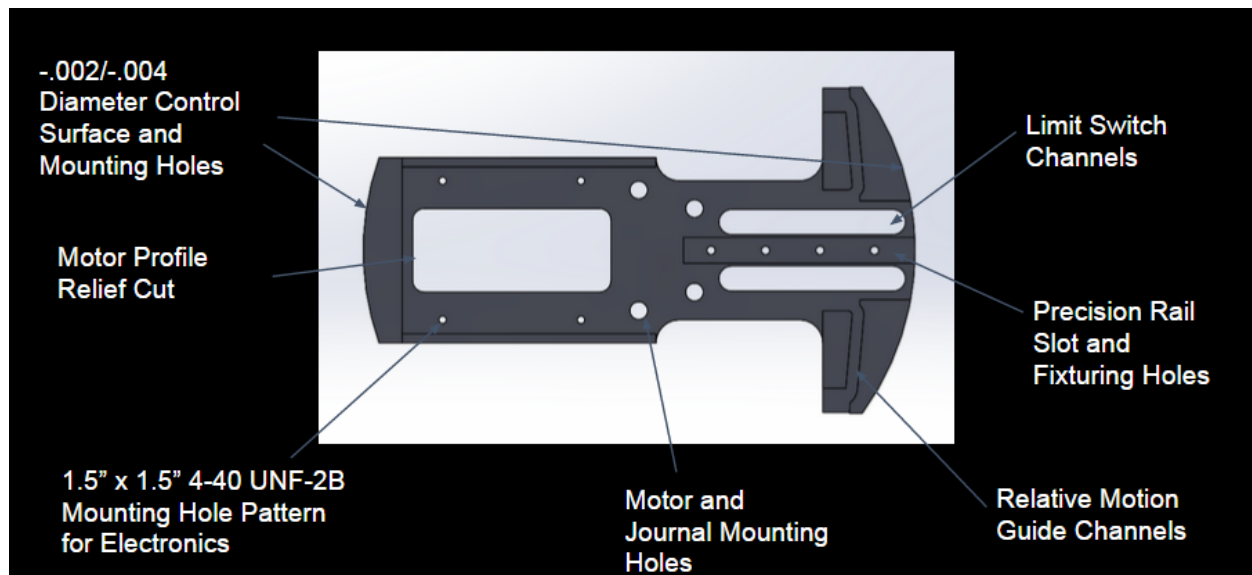


Figure 3A- Baseplate design showing many of the mentioned design features.

A pair of custom coupling rings was designed to interface with the NSR actuator and V-band. The male coupling ring is indexed with three female half inch alignment grooves around the surface which mates to the female NSR coupling ring. The female coupling ring contains 3 male tabs which interface with female grooves as well as holding a wave spring in place. The wave spring provides a kick-off force of approximately 88 lbf upon actuation. Both coupling rings have an outer diameter of 6.6 inches and an inner diameter of 6 inches outlined in the PDS. The coupling rings also exhibit the same internal structural features as the standard LV3 coupling ring modules and can thus be fitted to any standard LV3 coupling ring. This allows the NSR device to later be adapted to stage separation if PSAS decides to do so.

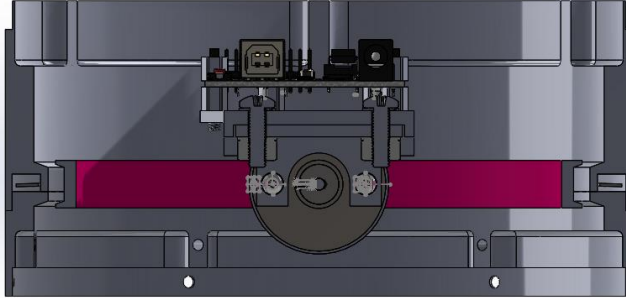


Figure 4A- A cutaway view of the NSR assembly including coupling rings and wave spring.

A prototype control system utilizing an Arduino Uno R3, a pair of limit switches, a button and a Monster Moto H-Bridge was developed for testing and demonstration purposes. The control system continuously samples a set of input pins for a state change to occur in the button. If a state change is sensed, the controller checks the status of each limit switch to determine the current position of the V-band. When the position has been detected, the controller then drives the motor in the direction needed to move the band toward the opposite limit switch. The controller then monitors the input pins for a second state change corresponding to the activation of the new limit switch. When the switch has been activated, the control board brakes the motor to the ground pin of the motor shield and control board.

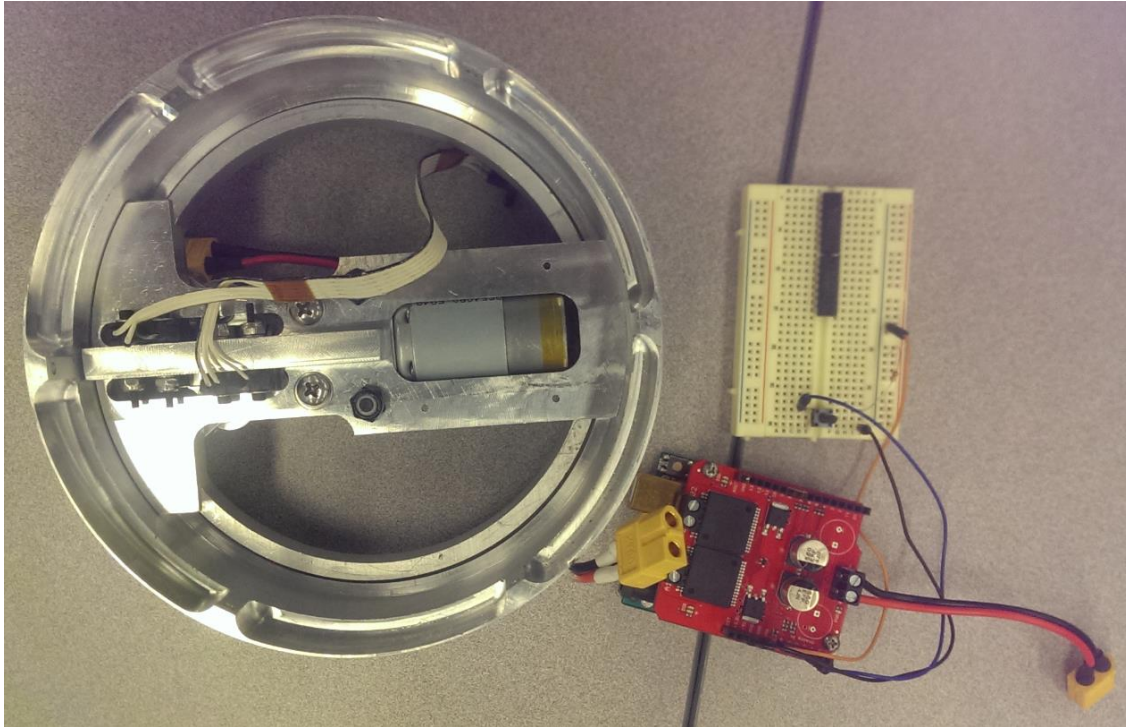


Figure 5A- Prototype control system of the NSR.

Appendix B: DFMEA on V-band

Components	Functions	Failure mode	Failure cause
clamp band	Provides clamping force	Cracking	Force exceeds ultimate strength
	Houses top and bottom ring together	plastic deformation	Force exceed yield strength
		nosecone comes off	insufficient clamping force
Top Ring	Provides surface for the clamping force	Cracking	Force exceeds ultimate strength
		nosecone doesn't come off	Friction too high
Bottom Ring	Provides surface for the clamping force	Cracking	Force exceeds ultimate strength
		nosecone doesn't come off	Friction too high
Step motor	Expands and contracts the metal band	motor doesn't engage	motor not strong enough
		Motor actuates early	No response
		Motor actuates late	Delayed response /early response
		motor comes loose off mounting	Screws back out or shear
	Receives electrical impulses from flight computer		Ratio for the motor size and power is incorrect
Quick release couplers (16 pin)	Decouples electricity	Stays connected	Tight fit
		No connection in the beginning	Corrosion
Battery	Provides electrical impulse to the step motor	battery leakage	Short circuit
		Dead battery	Quality of battery is not up to par Wasn't charged
Acme screw	Transmits motor torque into linear motion to provide clamping	Doesn't transmit motor torque	Threads get worn down
			Too much friction
		Cracks	Force exceeds ultimate strength
Ring retainer mechism	catches the clamp	Threads skip	Gear too small, pitch incorrect
		cracks	Force exceeds ultimate strength
Gear	Turns the Acme screw	Doesn't catch ring	Improperly sized
		Teeth strip	Materials are weak
Keyed alignment	Aligns top and bottom rings correctly	Too slow	Ratio for the motor size and power is incorrect
		Interface binds upon release	Force exceeds ultimate strength
		It doesn't fit	Tolerance/angle is incorrect
Kickoff springs (Optional)	Provides force for separation	It separates unevenly	Catches the quick release coupler
	Inside the guide pins	Not enough force separation	Springs yield Incorrect spring sizing

Severity	Occuranc	Detection	Rating of severity	Legend	Score
10	1	5	10.0	Harmful to persons	50
4	4	7	9.0	Harmful to persons	112
10	5	9	8.0	Permanently damages the rocket	450
4	1	5	7.0	Permanently damages the rocket	20
8	1	4	6.0	Moderately damages the rocket	32
4	1	5	5.0	Mildly damages the rocket	20
8	1	4	4.0	perminate replace of part	32
8	1	4	3.0	Small component which is replaceable needs rework	32
10	1	8	2.0	Small component which is replaceable gets damaged	80
8	7	8	1.0	Part wears down	448
8	5	8			320
5	1	2	Rating of occurrence		10
8	2	2			32
8	5	4	10.0	1 in 1 times	0
8	2	1	9.0	1 in 5 times	160
8	2	1	8.0	1 in 10 times	16
8	5	1	7.0	1 in 25 times	40
8	2	4	6.0	1 in 50 times	64
3	1	5	5.0	1 in 100 times	0
3	1	1	4.0	1 in 250 times	15
2	1	1	3.0	1 in 500 times	3
2	1	5	2.0	1 in 1000 times	10
2	3	2	1.0	1 in 2500 times	12
8	1	7			56
4	1	6	Detection Pre-flight		24
7	7	10			490
1	7	1	10	Hard to detect	7
3	7	1	9		0
4	4	5	8		21
			7		80
			6		
			5		
			4		
			3		
			2		
			1	Easy to detect	

Figure 1B: The DFMEA on the V-band which shows the three most critical failure modes.

Appendix C: Potential Yielding at Critical Point

A circular aluminum clamping mechanism (V-band) was tested to determine the force required to displace the band. A strain gauge was also mounted to the inside of the

band to measure stress at a critical location. This location was chosen because it was determined as the most critical point in the V-band. Stresses and displacements in the band were analysed prior to conducting the experiment using Abaqus Finite Element Analysis (FEA) software. The software was also used to determine the force required to displace the V-band to the maximum diameter. This testing was important due to the requirements brought by the PDS. The PDS requires the NSR to be quick to reset and quick to test, therefore the FEA software will tell the group the required forces and any possible yielding stresses in order to clamp the rings fully.

The dimensions, material, and change in clearance was known. The force and stress at critical points required to change the clearance 0.8 inches is desired to be known. There were three methods which were used, FEA half band, FEA full band and Castigliano's method. The main assumptions made were to try either the half band or the full band. The results showed to be closed to the actual readings as depicted in Table 1C. The experimental schematic could be seen in Figure 1C. While the two FEA analysis were depicted in Figure 2C.

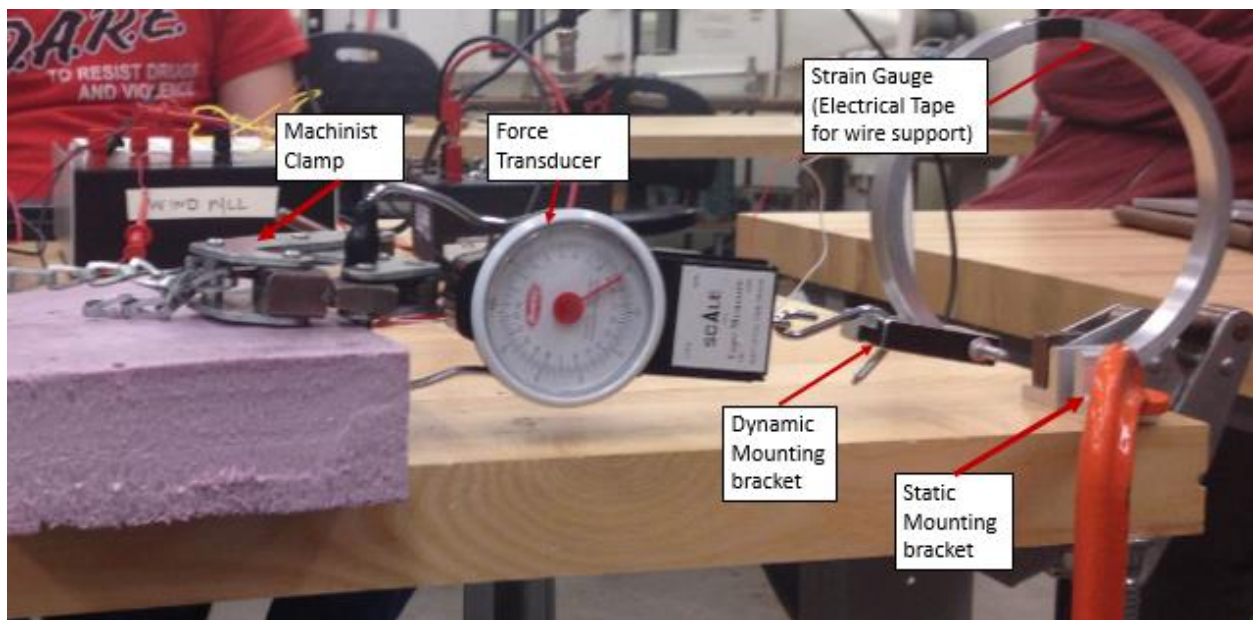


Figure 1C: The fixtures and apparatus of the experiment: note that the force exerted on the dynamic end of the V-band was in-line with the static end; i.e. the motion was constrained in one dimension. See appendix A for more details

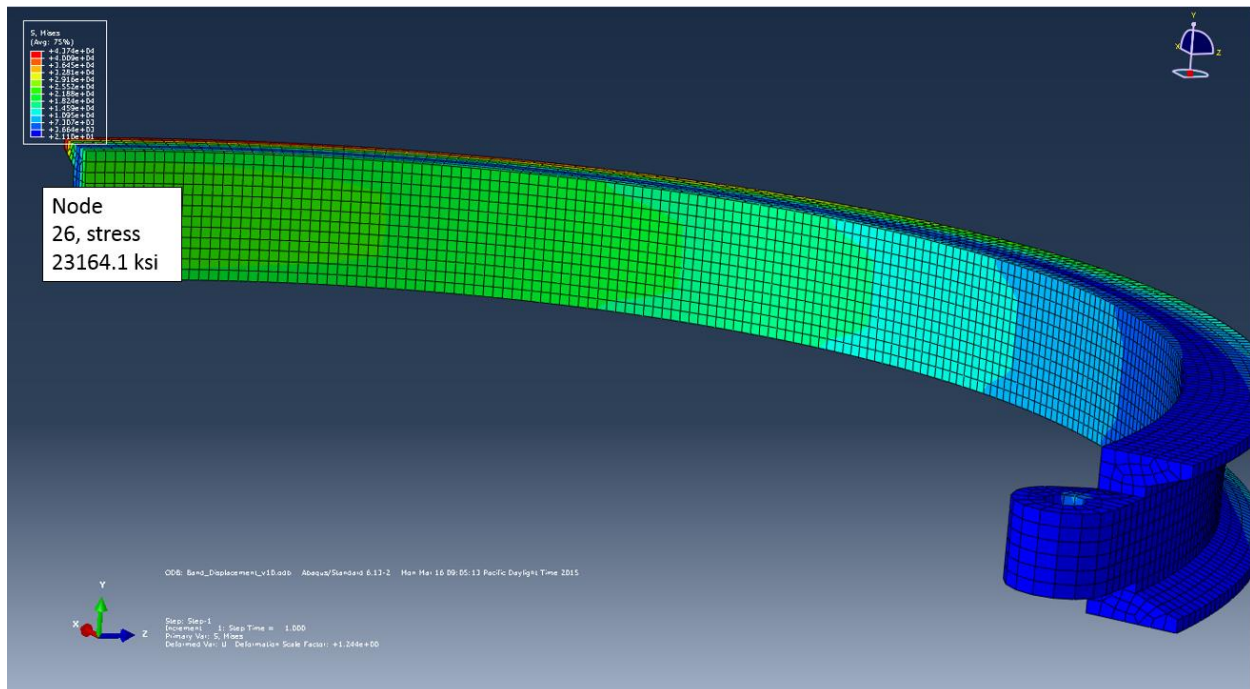


Figure 2C: FEA analysis of the half band shows the stress at the strain gauge.

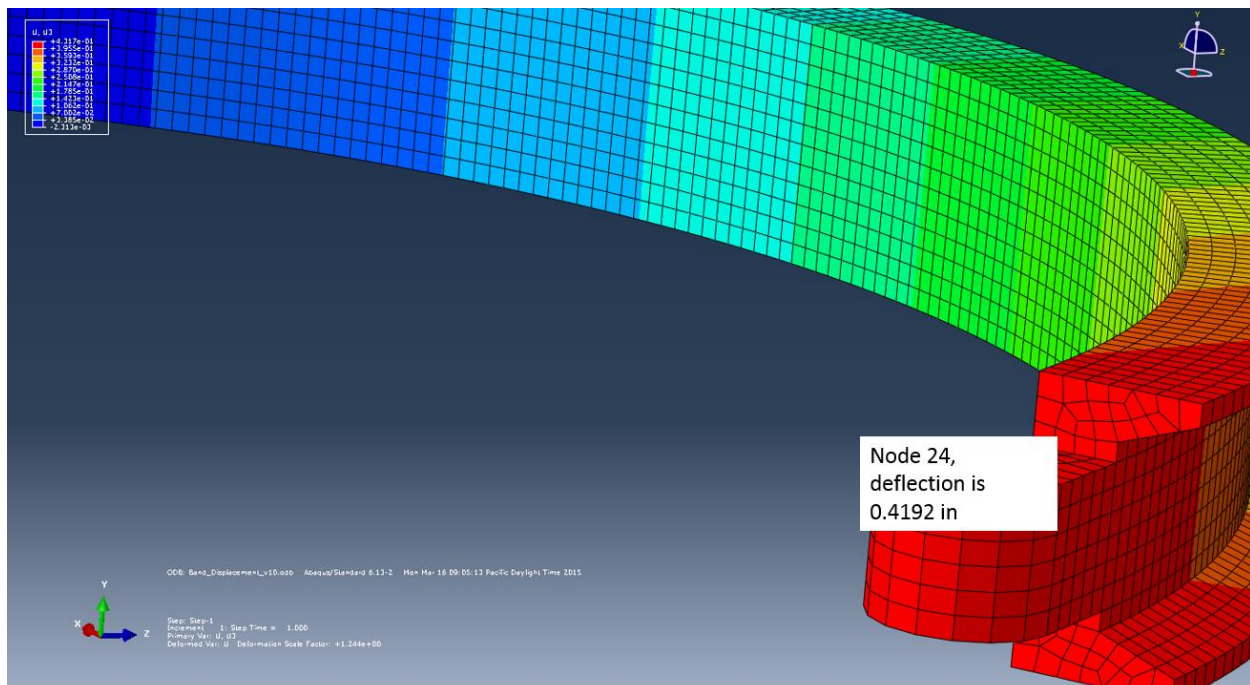


Figure 3C: The FEA analysis shows the deflection of the dynamic mounting bracket.

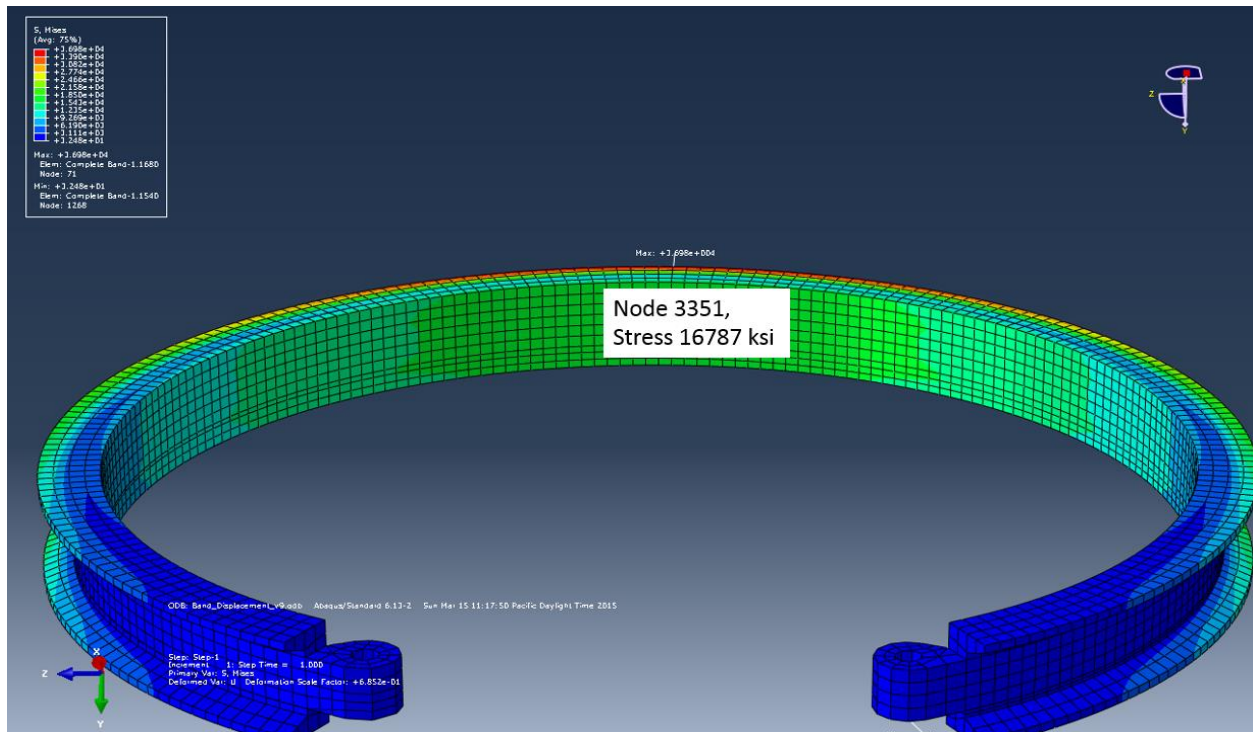


Figure 4C: The FEA analysis shows the stress of the full model being under 16.7 ksi of stress at the strain gauge.

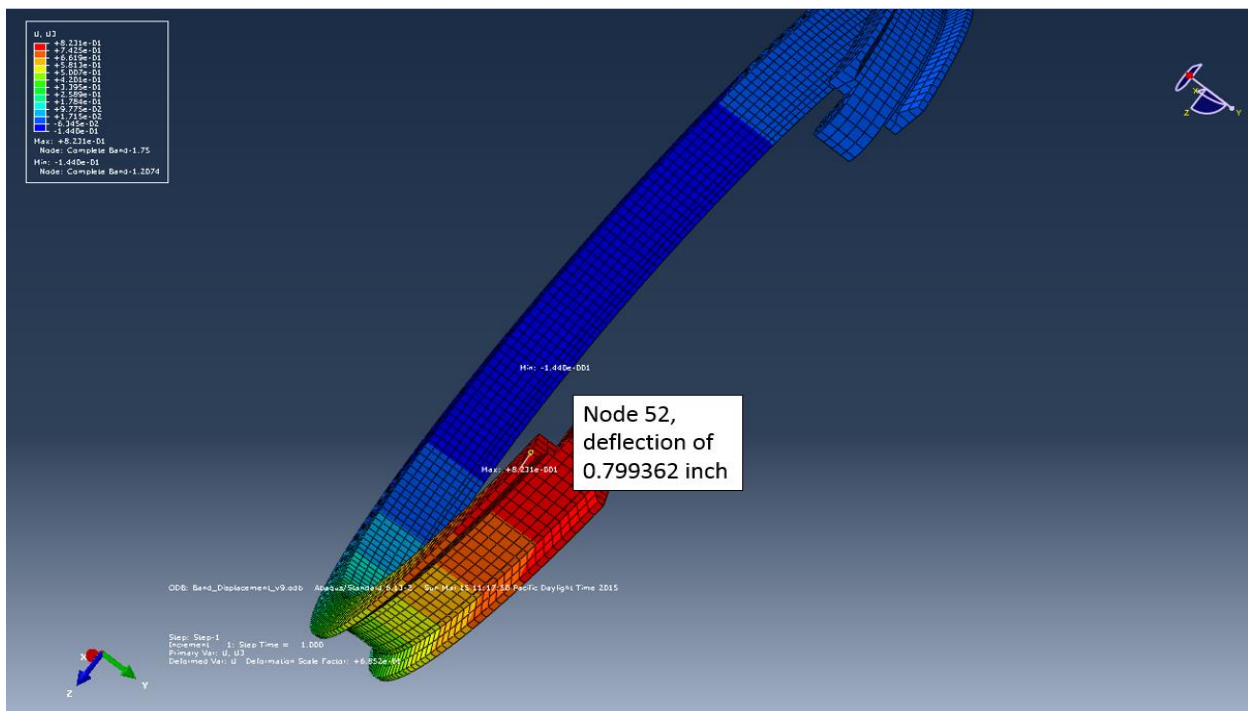


Figure 5C: The FEA analysis shows the amount of deflection at the dynamic mounting bracket.

Table 1C: The force required and stress generated in deflecting the V-band 0.8 in.

	Experimental	Castigliano's method	FEA: Full V-band Geometry	FEA: Half V-band geometry
Force to deflect V-band 0.8 in.	20.67 lbf	15.69 lbf	20.6 lbf	15.7 lbf
Stress at strain gauge location	27.90 ksi	N/A	16.79 ksi	23.16 ksi

Table 2C: Shows which methods had the lowest amount of error between each other in terms of force (lbf)

Percent error force required for V-band displacement	Experimental	Castigliano's method	FEA geometry full	FEA geometry half
Experimental	0	24%	0.3%	24%
Castigliano's method	24%	0	23.8%	23.7%
FEA geometry full	0.3%	23.8%	0	23.7%
FEA geometry half	24%	0.06%	23.7%	0

Table 3C: Shows which methods had the lowest amount of error between each other in terms of stress (ksi)

Percent error stress	Experimental	Castigliano's method	FEA geometry full	FEA geometry half
Experimental	0	N/A	39.8%	16.9%
Castigliano's method	N/A	N/A	N/A	N/A
FEA geometry full	39.8%	N/A	0	27.5%

FEA geometry	half	16.9%	N/A	27.5%	0
--------------	------	-------	-----	-------	---

The full band matched Castigliano's method, however the FEA half band matched the experimental reading better. Error was generated in multiple stages of the experiment. There was error in the readings from two key instruments, the digital caliper and the hanging scale. These instruments had an error of ± 0.001 in. and ± 0.5 lb. respectively. Over three trials, the average force required to deflect the V-band 0.8 in was found to be 20.67 lb_f, which agrees with a comparable FEA model.

Appendix D: Bill of Materials

Shown below is a table listing all of the parts that are included in the final assembly.

Table 1D: Bill of Materials (BoM) for all parts included in the final assembly

Part	Description	Location	QTY
E clips	1/8" E clips	Arms / sled, Arms / V-band	8
M2 x 8mm socket	M2 x 8mm socket screw	Sled assembly	4
7mm x 60mm rail	7mm x 60mm length precision rail	baseplate assembly	1
7mm carriage	7mm clean room carriage	baseplate assembly	1
1/8 x 3/8 x 5/32 bb	precision ball bearing	sled assembly	2
6-32 set screw	6-32 x .25	sled assembly	1
1/4-16 x .25 nut	ACME nut, 1/4/16	sled assembly	1
sled	custom machined sled	sled assembly	1
2-56 x .5 panhead	2-56 phillips panhead	baseplate assembly	3

limit switches	snap-action limit switch	baseplate assembly	2
3-56 x 1 socket	3-56 x 1 socket screw	baseplate assembly	4
3-56 washer	washer / spacer	baseplate assembly	8
3-56 lock nut	3-56 nylon lock nut	baseplate assembly	4
modular stem	custom machined stem	baseplate assembly	1
baseplate	custom machined baseplate	baseplate assembly	1
.25 x .678 thrust bearing	INA needle thrust bearing, .25	journal	2
.25 x .678 thrust washer	INA needle thrust washer, .25	journal	2
.175 x .125 coupler	custom machined coupler	journal	1
.25 collar	shaft collar	journal	1
1/4-16 ACME all thread	power screw	journal / drive train	2.5 in
journal	custom machined journal	journal	1
RS-550 motor	Banebots RS-550	motor assembly	1
motor mount	custom machined motor mount	motor assembly	1
M3 x 6mm	M3 x 6mm machine screw	motor assembly	2
10-32 x 5/8	10-32 machine screw	actuator assembly	2
10-32 x 3/8	10-32 machine screw	actuator assembly	2
10-32 lock nut	10-32 nylon lock nut	actuator assembly	2
relative motion arms	custom machined arms	actuator assembly	2
dowel pin size 1	custom dowel pin, size 1	actuator assembly	2
dowel pin size 2	custom dowel pin, size 2	actuator assembly	2
V-band	custom machined band clamp	actuator assembly	1
wave spring	smalley SSR-0637	coupling rings	1
index tabs	custom machined tabs	coupling rings	3
4-40 x .25	4-40 x .25 tapered machine	coupling rings	3

	screws		
male coupling ring	custom coupling ring	coupling rings	1
female coupling ring	custom coupling ring	coupling rings	1
4-40 x .5	4-40 x .5 tapered machine screws	coupling rings	7

Appendix E: Analysis Based Design Decisions

Castigliano's For V-band

Summary: The objective of this analysis is to find the amount of force required to open the v-band sufficiently for full clamping. The analysis uses Castigliano's theorem to find that 15.6lb of force is needed to open the band .8 in. These results are less than the experimental value and value found by FEA, but still within reason. [1]

Castiglianos analysis for beam deflection on flex band:

$$M = F \cdot R \cdot \cos(\theta)$$

$$F_{\theta} = F \cdot \cos(\theta)$$

$$F_r = F \cdot \sin(\theta)$$

$$\frac{dF_{\theta}}{dF} = \cos(\theta)$$

$$\frac{dF_r}{dF} = \sin(\theta)$$

$$\frac{dM}{dF} = R \cdot \cos(\theta)$$

$$\frac{dM \cdot F_{\theta}}{dF} = 2 \cdot F \cdot R \cdot \cos^2(\theta)$$

$$U_1 = \int \frac{M^2}{2 \cdot A \cdot e \cdot E} d\theta \quad U_2 = \int \frac{F_{\theta}^2 \cdot R_{\text{curve}}}{2 \cdot A \cdot E} d\theta$$

$$U_3 = \int \frac{M \cdot F_{\theta}}{A \cdot E} d\theta \quad U_4 = \int \frac{C_c \cdot F_r^2 \cdot R_{\text{curve}}}{2 \cdot A \cdot G_{al}} d\theta$$

because $R/h > 10$, eccentricity does not apply. U_1 is then estimated as:

$$U_1 = \int \frac{M^2 \cdot R_{\text{curve}}}{2 \cdot E \cdot I_{y,\text{channel}}} d\theta$$

Assumptions:

$C_c := 1.0$ C is a cross-sectional correction factor, see Table 4-1 in Shigley's, page 163

Material is aluminum T-6061:

$$E := 68.9 \text{ GPa} \quad G_{Al} := 26 \text{ GPa}$$

Model properties:

$$R_{curve} := \frac{5.21}{2} \text{ in} = 2.605 \text{ in} \quad A_{beam} := 2 \cdot .15 \text{ in} \cdot .19 \text{ in} = 3.677 \times 10^{-5} \text{ m}^2$$

$$e_c = R - r_n \quad \text{eccentricity term (not used, see above)}$$

$$\text{Disp} := 0.4346 \text{ in}$$

$$\text{Arc}_{curve} := 180 \text{ deg} - 25.37 \text{ deg} = 154.63 \text{ deg} \quad \text{going from } 25.37 \text{ deg to } 180 \text{ deg}$$

$$I_{y,channel} = \frac{1}{3} \left[2 \cdot s_{channel} \cdot b_{channel}^3 + t_{channel} \cdot t_{channel}^3 + \frac{s_{channel}}{2} \cdot (b_{channel}^4 - t_{channel}^4) \right] - A_{channel} (b_{channel} - y_{channel})^2$$

$$a_{channel} := 0.14 \text{ in} \quad y_{channel} := 0.2554 \text{ in} \quad h_{channel} := 0.44 \text{ in}$$

$$t_{channel} := 0.15 \text{ in} \quad l_{channel} := 0.37 \text{ in}$$

$$b_{channel} := 0.29 \text{ in} \quad n_{channel} := .0704 \text{ in}$$

$$s_{channel} := 0.0433 \text{ in} \quad d_{channel} := 2 \cdot y_{channel} = 0.511 \text{ in}$$

$$A_{channel} := d_{channel} \cdot t_{channel} + a_{channel} (s_{channel} + n_{channel}) = 0.093 \text{ in}^2$$

$$s_{channel} := \frac{h_{channel} - l_{channel}}{2(b_{channel} - t_{channel})} = 0.25$$

$$I_{y,channel} := \frac{1}{3} \left[2 \cdot s_{channel} \cdot b_{channel}^3 + t_{channel} \cdot t_{channel}^3 + \frac{s_{channel}}{2} \cdot (b_{channel}^4 - t_{channel}^4) \right] - A_{channel} (b_{channel} - y_{channel})^2 = 1.283 \times 10^{-3} \cdot \text{in}^4$$

setup of problem:

$$U_{\text{tot}} = U_1 + U_2 + U_3 + U_4 \quad \text{from castiglianos:} \quad \text{Disp} = \frac{\delta U_{\text{tot}}}{\delta F}$$

$$\text{Disp} = \int \frac{M \cdot R_{\text{curve}}}{2 \cdot E \cdot I_{y,\text{channel}}} \left(\frac{dM}{dF} \right) d\theta + \int \frac{F_{\theta} \cdot R}{A \cdot E} \left(\frac{dF_{\theta}}{dF} \right) d\theta + \int \frac{1}{A \cdot E} \left(\frac{d(M \cdot F_{\theta})}{dF} \right) d\theta + \int \frac{C_c \cdot F_r \cdot R}{A \cdot G} \left(\frac{d \cdot F_r}{dF} \right) d\theta$$

$$\text{Disp} = \frac{F \cdot R^3}{2 \cdot E \cdot I_{y,\text{channel}}} \cdot \int_{25.37}^{180} \cos^2(\theta) d\theta + \frac{F \cdot R}{A \cdot E} \cdot \int_{25.37}^{180} \cos^2(\theta) d\theta + \frac{2 \cdot F \cdot R}{A \cdot E} \cdot \int_{25.37}^{180} \cos^2(\theta) d\theta + \frac{F \cdot R}{A \cdot G} \cdot \int_{25.37}^{180} \sin^2(\theta) d\theta$$

$$\text{Solving integral term:} \quad \int_{25.37}^{180} \cos^2(\theta) d\theta = 77.4405 \quad \int_{25.37}^{180} \sin^2(\theta) d\theta = 77.1895$$

$$\text{Disp} = 77.4405 \cdot \left(\frac{F \cdot R^3}{2 \cdot E \cdot I_{y,\text{channel}}} + \frac{F \cdot R}{A \cdot E} + \frac{2 \cdot F \cdot R}{A \cdot E} \right) + 77.1895 \cdot \left(\frac{F \cdot R}{A \cdot G} \right)$$

factor out F from all terms, solve for F with known displacement:

$$\text{Disp} = F \cdot \left[77.4405 \cdot \left(\frac{R^3}{2 \cdot E \cdot I_{y,\text{channel}}} + \frac{R}{A \cdot E} + \frac{2 \cdot R}{A \cdot E} \right) + 77.1895 \cdot \left(\frac{R}{A \cdot G} \right) \right]$$

$$F_1 := \frac{\text{Disp}}{\left[77.4405 \cdot \left(\frac{R_{\text{curve}}^3}{2 \cdot E \cdot I_{y,\text{channel}}} + \frac{R_{\text{curve}}}{A_{\text{beam}} \cdot E} + \frac{2 \cdot R_{\text{curve}}}{A_{\text{beam}} \cdot E} \right) + 77.1895 \cdot \left(\frac{C_c \cdot R_{\text{curve}}}{A_{\text{beam}} \cdot G_{\text{al}}} \right) \right]} = 34.908 \cdot \text{N}$$

$$F_1 = 7.848 \cdot \text{lbf}$$

Calculating for yield of designed clamping area

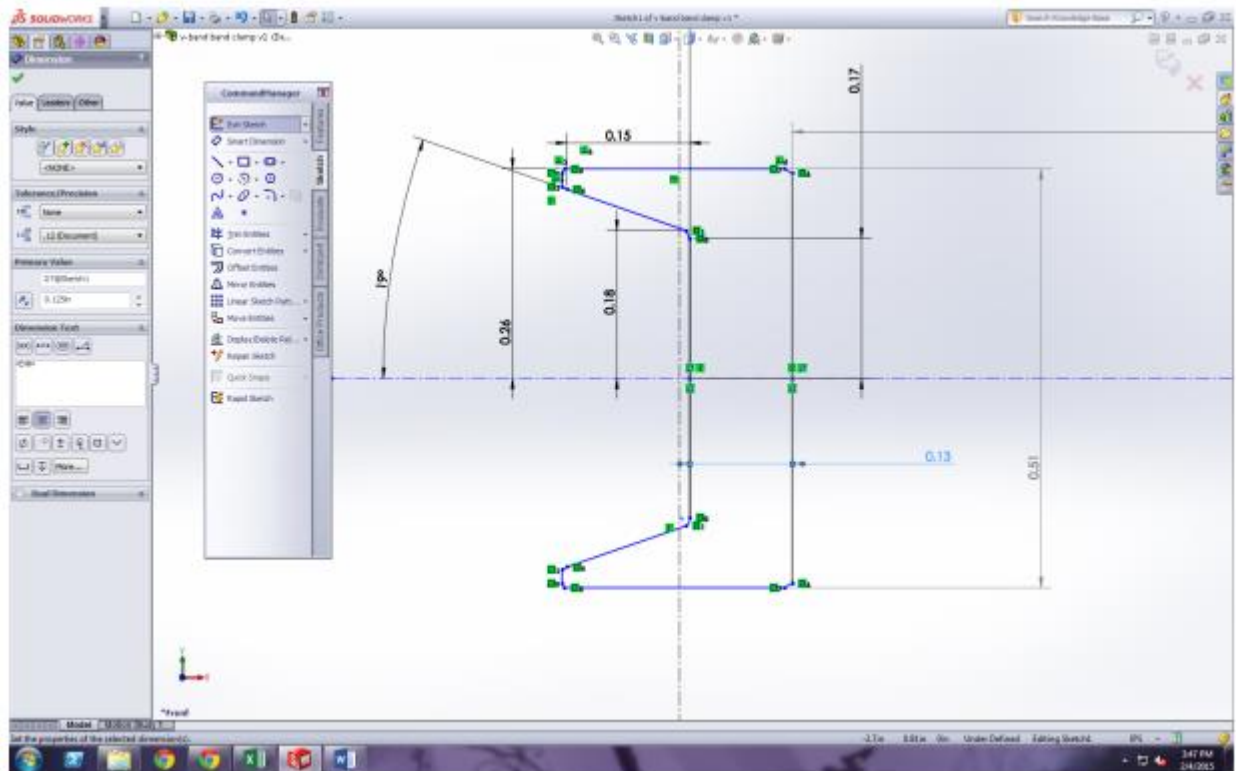


Figure 1E- Cross section of v-band.

Summary: The objective of this analysis is to find the minimum wall thickness of the V-band to withstand the forces outlined in the PDS. The PDS states that the device needs to withstand a minimum tensile force of 250 lbf.

Determining if the smallest cross sectional area of the design will yield.

After more research, we found that a 250 lb tensile load is a better theoretical value versus 750 lb that was used to calculate the wall thickness.

Tensile force $F_t := 250\text{ lbf}$

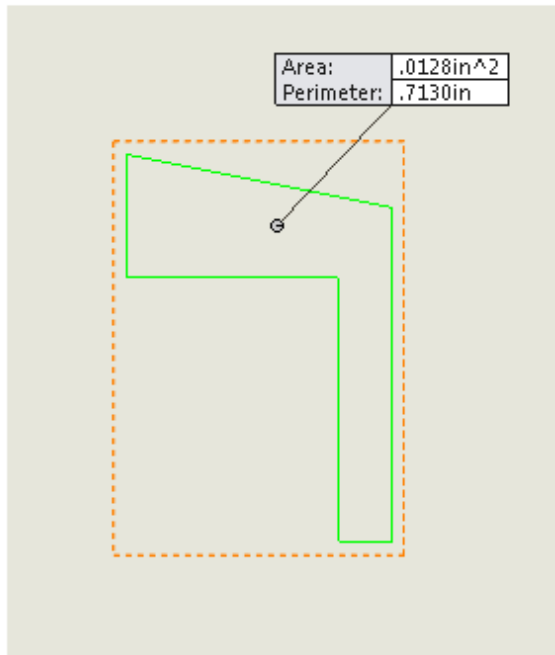
Angle of attack $\theta := 20\text{ deg}$

Reaction force $F_r := F_t \cdot \cos(\theta)$ $F_r = 234.923\text{ lbf}$

Yield strength of T-6 6061 aluminum $\sigma := 40000\text{ psi}$

Minimum cross sectional area required with a 250lb tensile load

$$\text{areamin} := \frac{F_r}{\sigma} \quad \text{areamin} = 5.873 \times 10^{-3} \cdot \text{in}^2$$



Smallest cross sectional area of design $\text{xarea} := 0.0128\text{ in}^2$

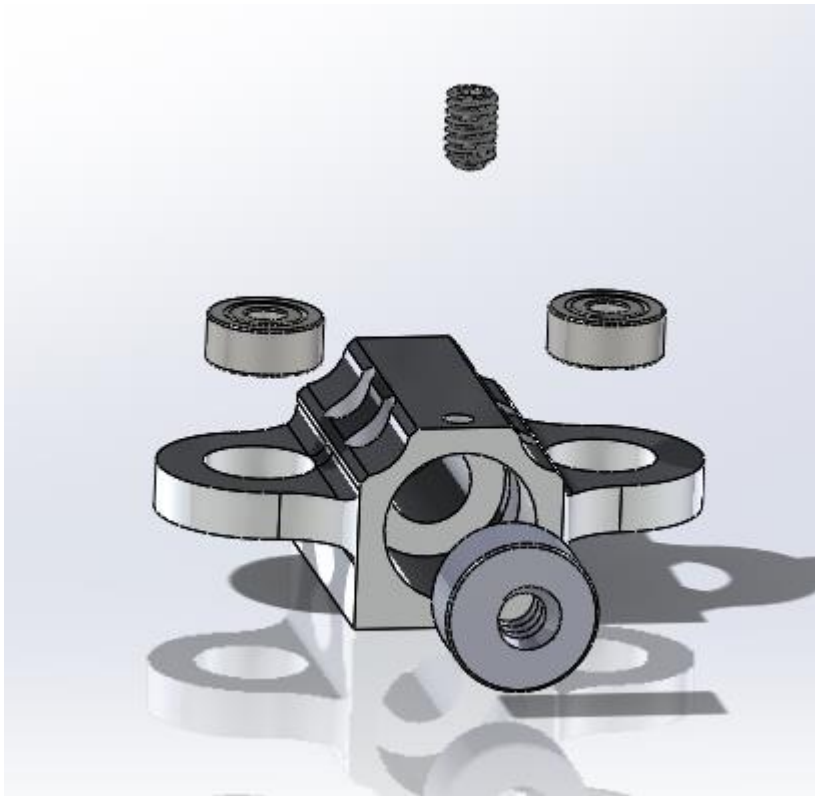
Analysis shows that the cross sectional area of the clamping surface will not yield at a tensile load of 250 lb.

+

APPENDIX F: Assembly Instructions

Sled Sub-Assembly

Part	Qty	Description
1	1	Sled
2	2	1/8" ID x 3/8" OD Bearing
3	1	1/4-16 x .25" ACME Nut
4	1	6-32 Set Screw



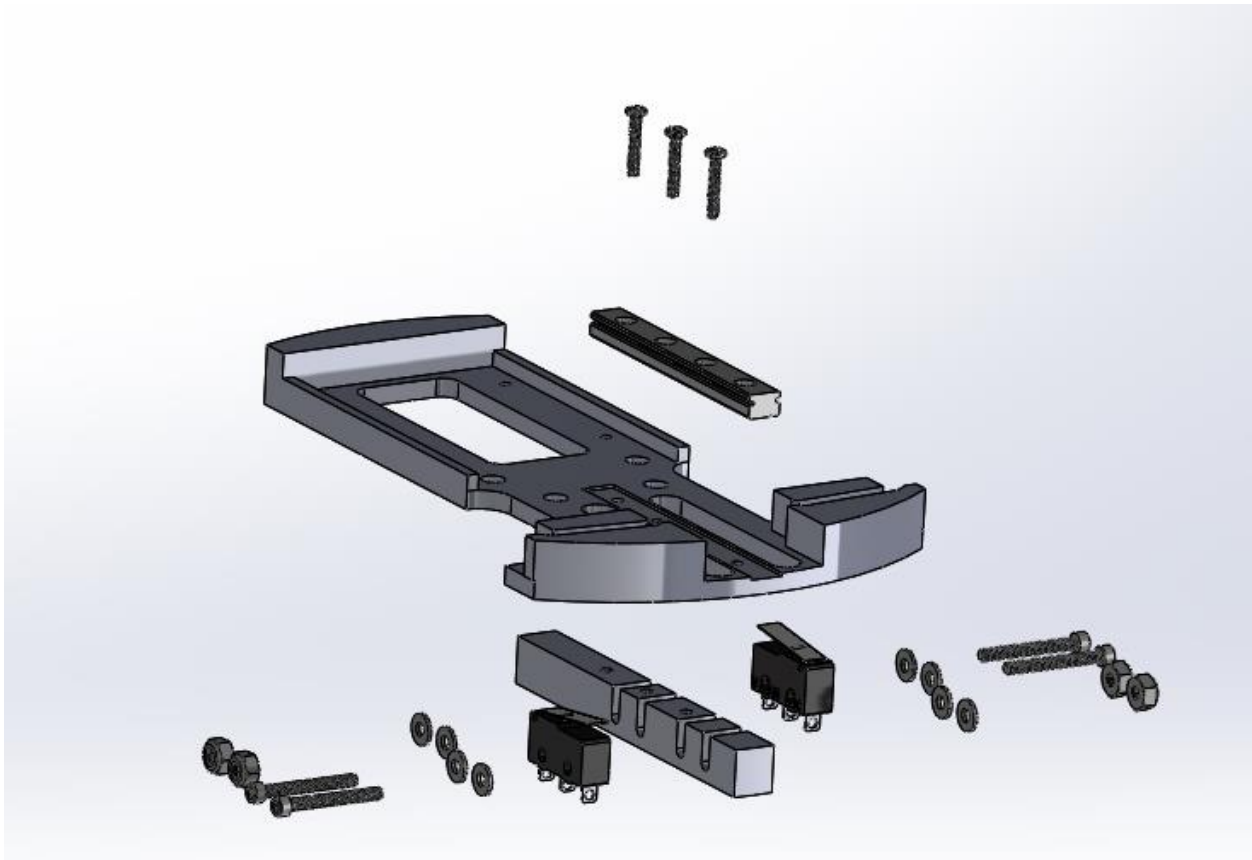
Instructions:

1. Using an arbor press, press both bearings into the holes along the side of the sled.
Press the 1/4-16 ACME Nut into the counterbore on the front surface of the sled.

2. Place some Loctite onto the threads of the 6-32 Set Screw. Screw the set screw through the hole located in the top of the sled until it is snug against the ¼-16 ACME Nut.

Baseplate Sub-Assembly

Part	Qty	Description
1	1	Baseplate
2	3	2-56 x .5" Phillips Panhead Machine Screws
3	2	Limit Switches
4	4	#3 x 1" Socket Head Cap Screws
5	8	#3 Nylon Lock Nuts
6	8	#3 Washers
7	1	7mm x 60mm Precision Guide Rail
8	1	Modular Baseplate Stem

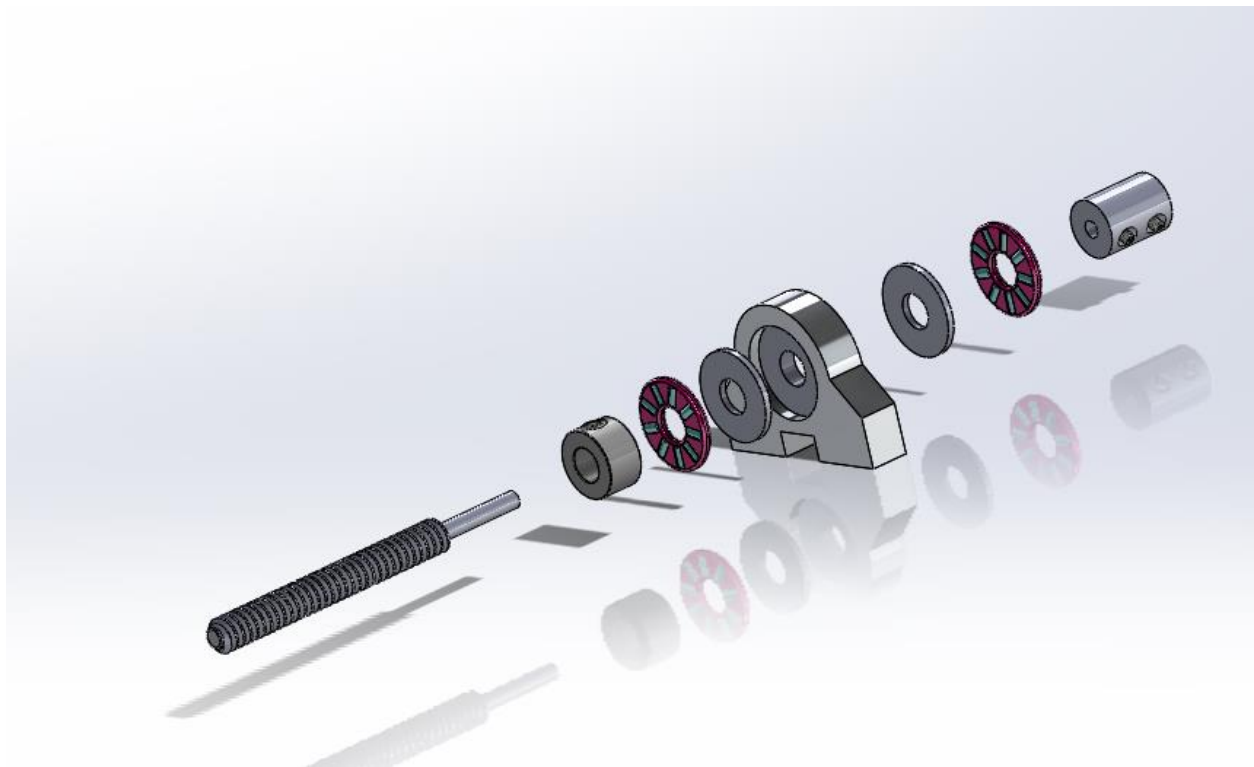


Instructions:

1. Slide the 7mm Precision Guide Rail into the slot for the guide rail.
2. Place Modular Baseplate Stem on the bottom of the baseplate and attach the stem and rail using the 3 2-56 x .5" Phillips Panhead screws.
3. Align the rear limit switch with the left hand side of the Modular Baseplate Stem grooves as shown.
4. Thread two #3 screws with washers through the limit switch and Stem grooves. Place a second set of washers on the exposed end of the screws.
5. Thread two #3 Nylon Lock Nuts over the exposed ends of the screws. Tighten the nuts down most of the way, but leave some play in the limit switches for later adjustment.
6. Repeat steps 3 through 5 for the front limit switch, but with the switch facing the opposite way and in with the switch aligned to the forward most groove set of the Modular Baseplate Stem.

Drive Train Sub-Assembly

Part	QTY	Description
1	1	Journal
2	2	INA 0.25 ID x 0.688 OD Needle Thrust Bearings
3	2	INA 0.25 ID x 0.688 OD Thrust Washers
4	1	0.125" x 0.125" Shaft Coupler
5	1	0.25" Shaft Collar
6	1	1/4-16 x 2.75" Length ACME Power Screw



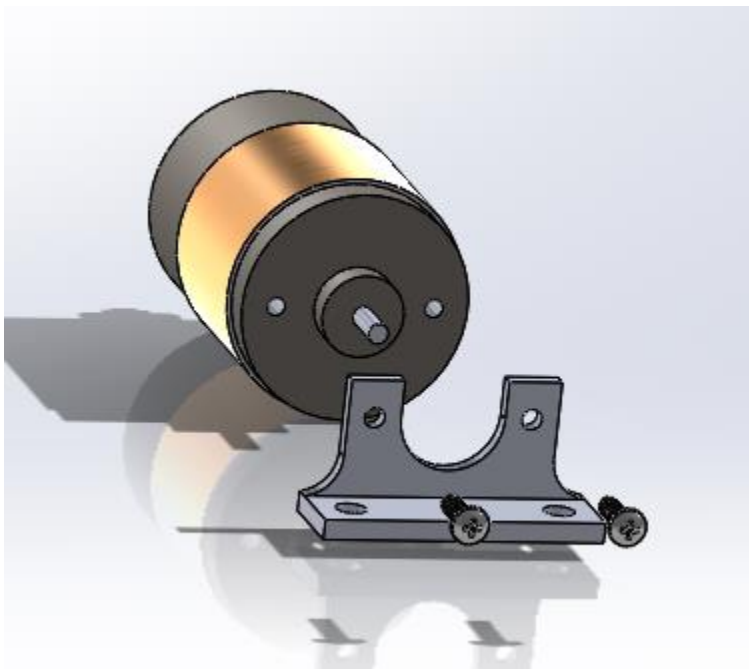
Instructions:

1. Seat one Thrust Washer and one Needle Thrust Bearing into the Journal.
2. Seat the 0.25" Collar onto the ACME Power screw approximately 2.25" down the shaft from the unturned side.
3. Slide the power screw through the journal and bearing assembly until the 0.25" Collar is seated against the Needle Thrust Bearing.
4. Repeat step one for the other side of the Journal.
5. Seat the 0.125" to 0.125" Shaft Coupler over the turned side of the 1/4-16 ACME Power Screw until the Shaft Coupler makes contact with the second Needle Thrust Bearing.

6. Tighten down all set screws. Apply Loctite to all threaded joints if connections feel loose or worn.

Motor Mount Sub-Assembly:

Part	QTY	Description
1	1	BaneBots RS-550 Brushed DC Motor
2	1	Motor Mounting Bracket
3	2	M3 x 6mm Machine Screws

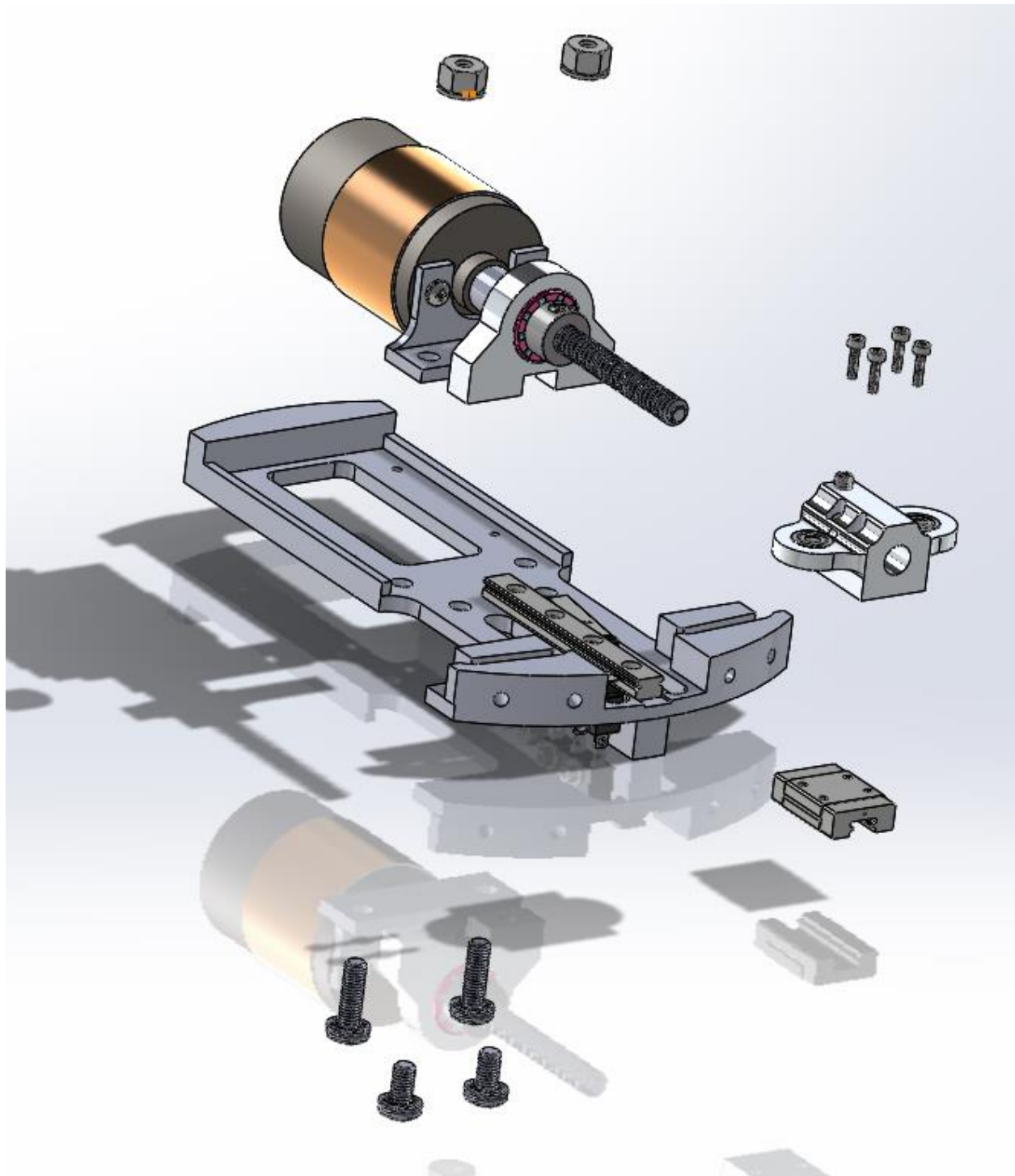


Instructions:

1. Align the metric 3 mounting holes on the BaneBots RS-550 DC motor with the mounting holes on the Motor Mounting Bracket.
2. Screw the Motor Mounting Bracket to the DC motor with the two M3 x 6mm Machine Screws.

Actuator Sub-Assembly:

Part	QTY	Description
1	1	Motor Mount Sub-Assembly
2	1	Power Train Sub-Assembly
3	2	10-32 x 5/8" Length Machine Screws
4	2	10-32 x 3/8" Length Machine Screws
5	1	7mm Precision Carriage
6	4	M2 x 8mm Socket Headcap Screws
7	2	10-32 Nylon Lock Nuts
8	1	Baseplate Sub-Assembly
9	1	Sled Sub-Assembly



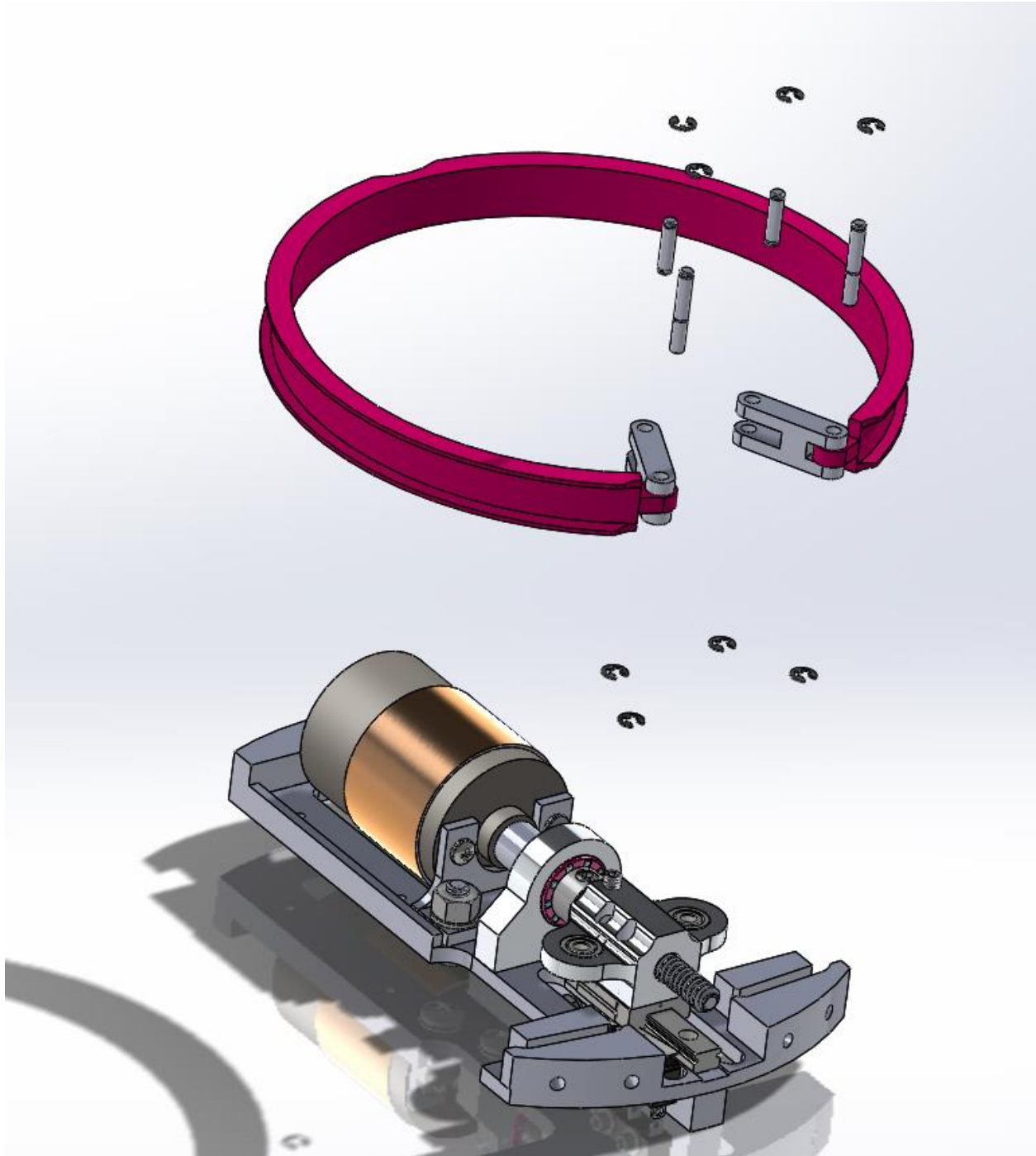
Instructions:

1. Screw the Sled Sub-Assembly onto the 7mm Precision Carriage (5) using the M2 x 8mm socket headcap screws (6).
2. Slide the motor shaft into the free side of the shaft coupler (located on the drive train sub-assembly).
3. align the 10-32 threaded mounting holes of both the motor mount and the journal with the 10-32 mounting holes on the baseplate.

4. Thread the $\frac{3}{8}$ " length 10-32 screws into the Journal. Leave them Hand tight for now.
5. Slide the $\frac{5}{8}$ " length 10-32 screws through the motor mount holes and thread the 10-32 nylon lock nuts over the top of the screws. Leave them hand tight for now.
6. Depress the lever of the front limit switch with a flathead screw driver or small allen key.
7. With the limit switch lever depressed, slide the sled and 7mm carriage assembly onto the 7mm precision rail. **CAUTION: the limit switch can be easily damaged in this step. Additionally, the 7mm carriage contains dozens of 1/32" ball bearings in the bottom of it which can easily come out if the assembly is jarred. Take care in this step and be careful not to damage the components.**
8. With the limit switch depressed and the sled assembly partially on the rail, hand turn the power screw until the entire sled assembly is on the rail and has cleared the front limit switch.
9. Tighten all screws and nuts using the appropriate tools. Tighten the set screws on the shaft coupler last. When tightening screws on the shaft coupler, rotate the power screw several times to ensure that the screw is aligned well and does not have any rough spots throughout its rotation.

Attaching the V-band to the Actuator Sub-Assembly:

Part	QTY	Description
1	1	Actuator Sub-Assembly
2	2	Dowel Pin Size 1
3	2	Dowel Pin Size 2
4	8	1/8" E Clips
5	1	V-Band
6	2	0.8" Relative Motion Arms



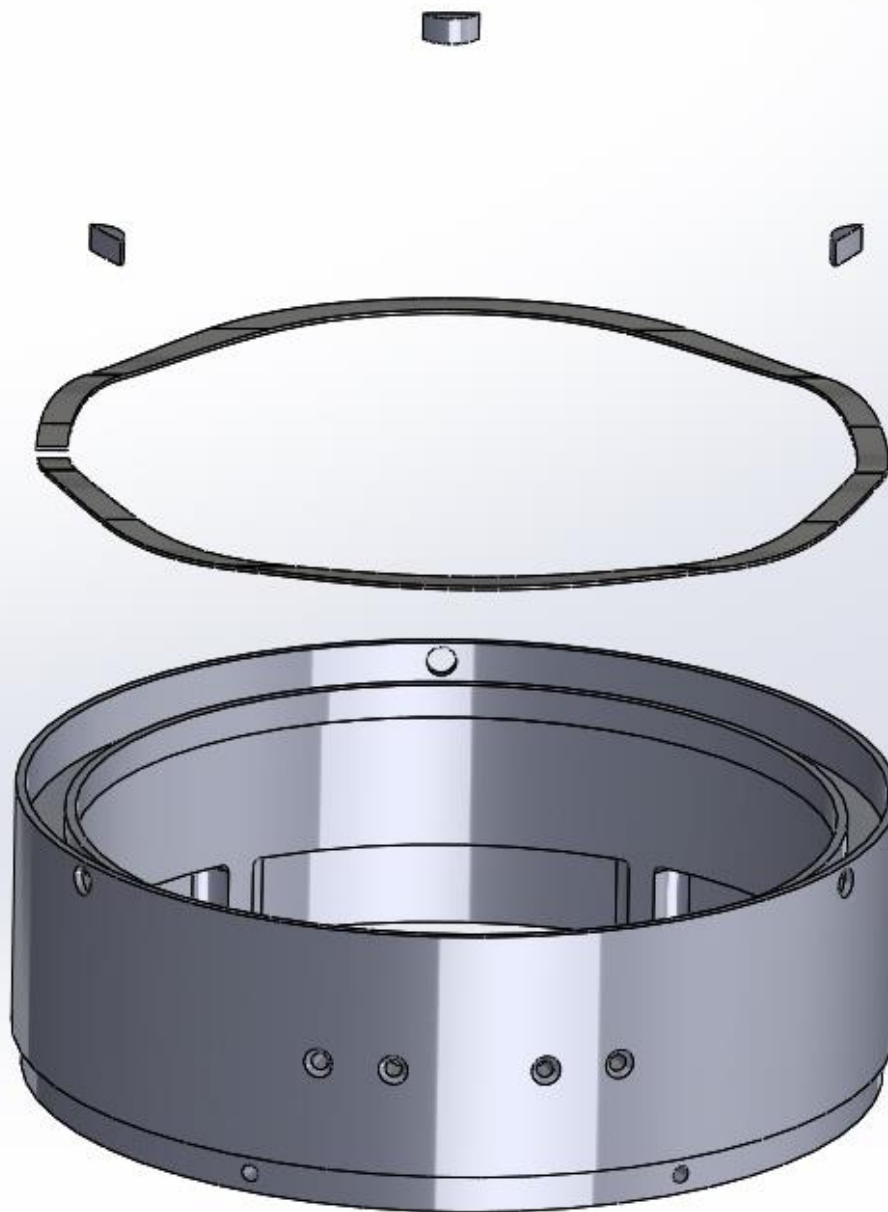
Instructions:

1. Attach one E Clip to the top side of each of the Size 2 Dowel Pins (the longer of the two).
2. Slide the front side (the front side has the shorter groove) of one of the relative motion arms over the connection tab of the V-band.
3. Slide one of the Size 2 Dowel Pins through the relative motion arm and V-band tab.
4. repeat steps 2 and 3 for the other relative motion arm and V-band tab.
5. Flip the V-band over and attach a second E Clip to the bottom of the dowel pin size 2.

6. Slide the V-band and relative motion arm assembly over the actuator sub-assembly. The exposed length of the dowel pins should seat into the guide rails of the baseplate.
7. Rotate the back side of the relative motion arms until the second set of holes lines up with the bearing holes in the sled.
8. Attach an E Clip to one side of each of the dowel pin size 1 pins.
9. Slide the pins through the relative motion arms and bearings.
10. Flip the assembly over and attach the last two E clips the the bottom side of the dowel pin size 1. Note: the bottom E Clips are very difficult to seat over the dowel pins and will test the patience of any mortal.

Male Coupling Ring and Wave Spring Sub-Assembly

Part	QTY	Description
1	3	Indexing Tabs
2	1	Male Coupling Ring
3	1	Wave Spring (Smalley Springs SSR-0637)
4	3	4-40 x 0.25" Tapered Machine Screws



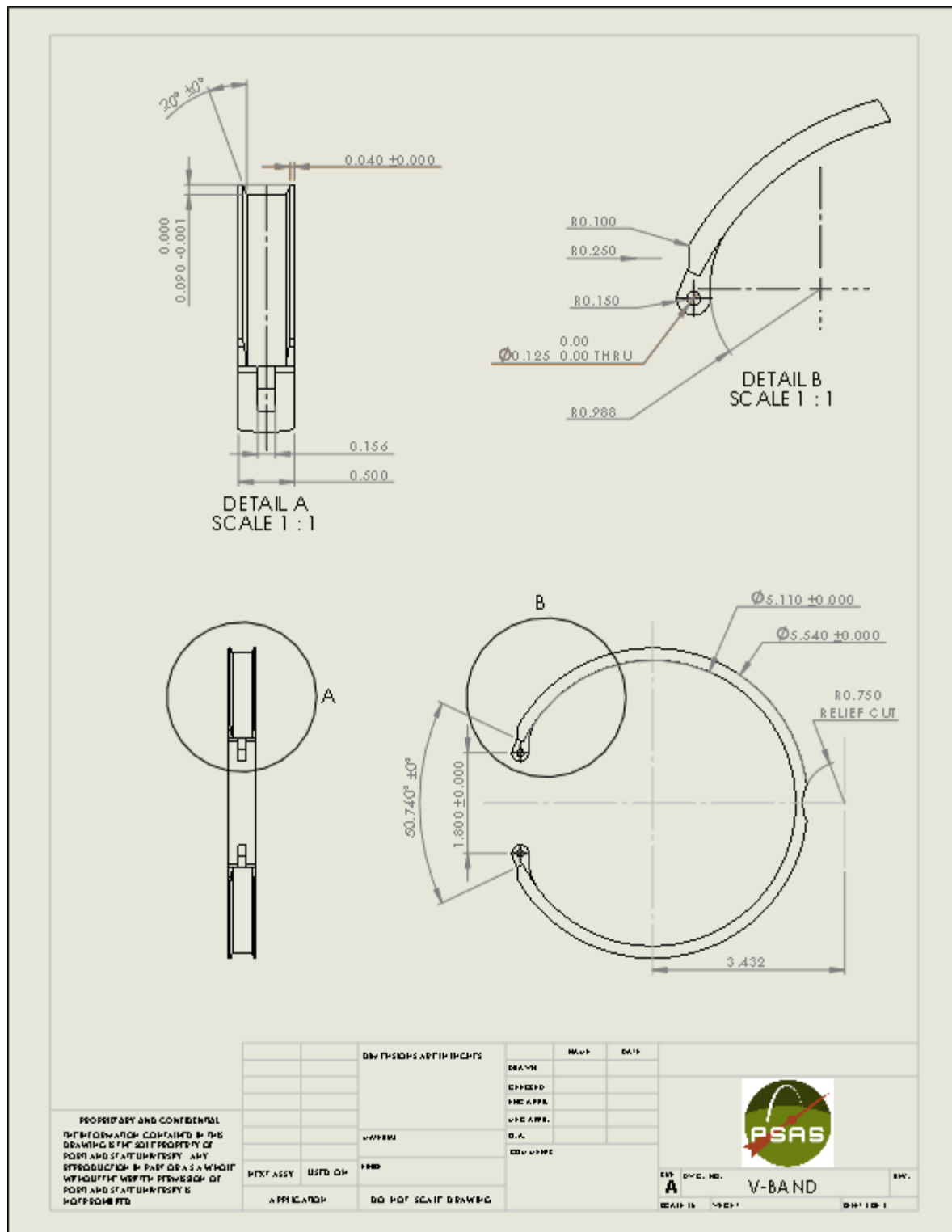
Instructions:

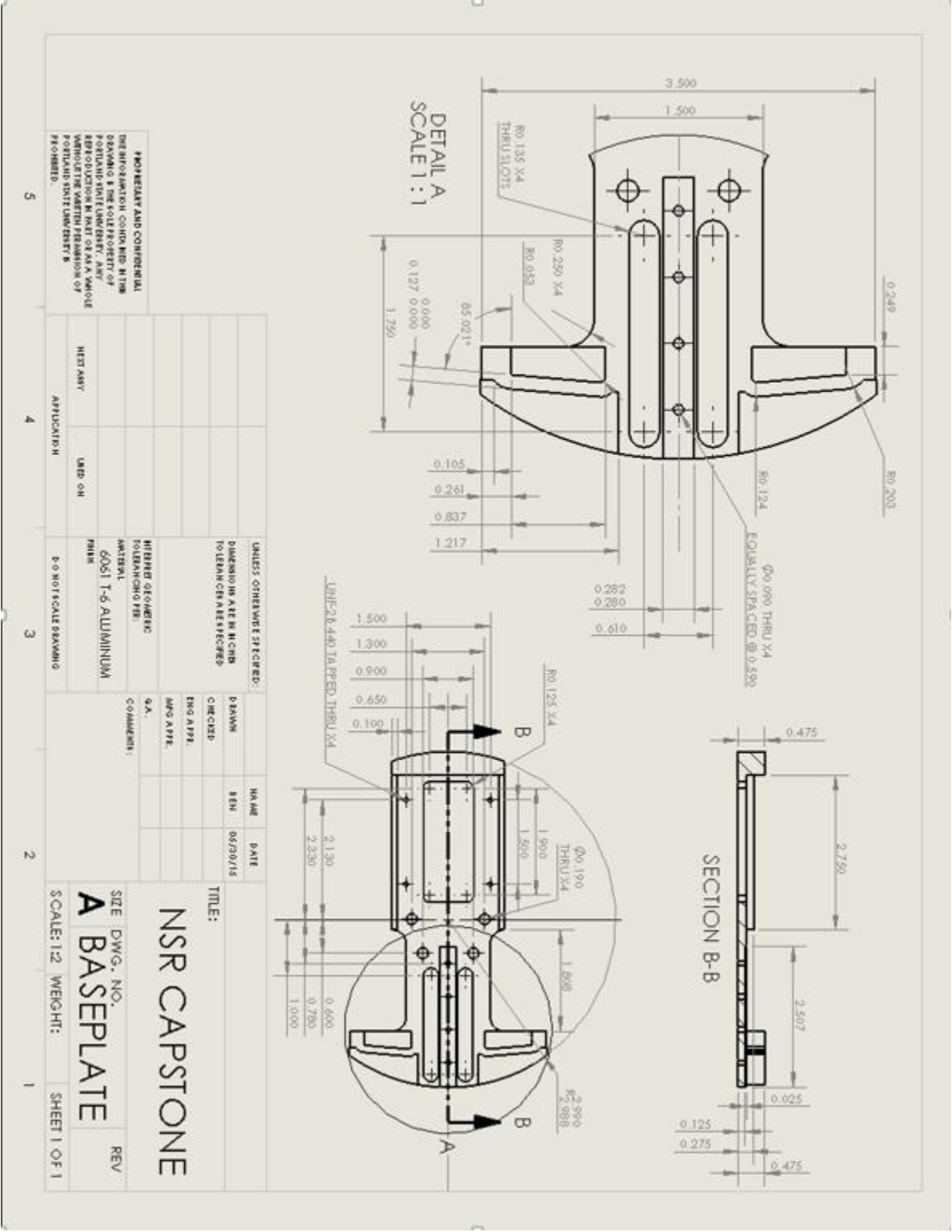
1. Place the wave spring in the groove of the male coupling ring.
2. Place the indexing tabs over the wave spring and line them up with the three holes in the side wall of the coupling ring.
3. Screw the 4-40 x 0.25" tapered machine screws into the side wall of the coupling ring. This will secure the wave spring into the provided groove.

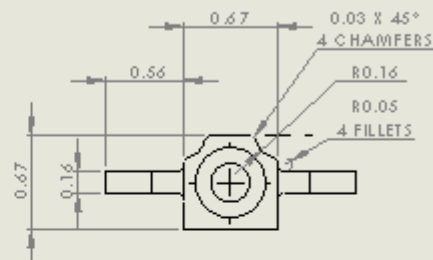
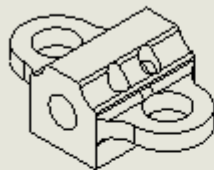
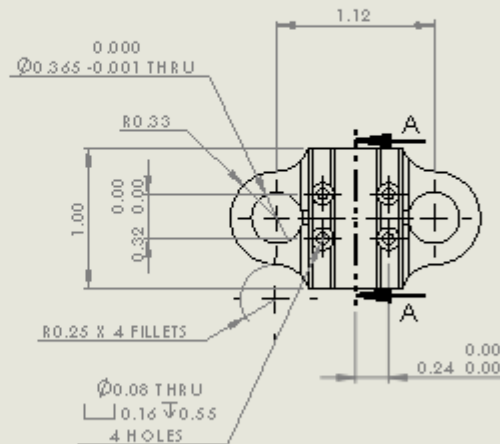
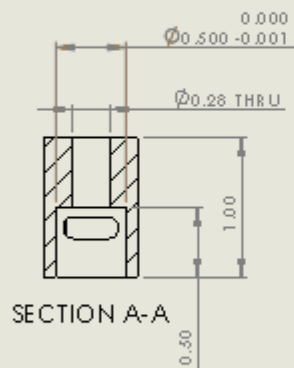
Seating the Actuator and V-band Assembly into the Coupling Ring

The actuator and V-band assembly is fixed to the male coupling ring and wave spring assembly by seven 4-40 tapered machine screws. When seating the actuator assembly inside the male coupling ring assembly, gently thread all screws in until they are hand tight, alternating between the front four screws and back three screws. Gently tighten all screws down with an allen key only after all screws have been seated and are hand tight. Connect all electronics at this time. The actuator and male coupling ring assembly is now flight ready, and can be mated with the female coupling ring.

Appendix G: Drawings





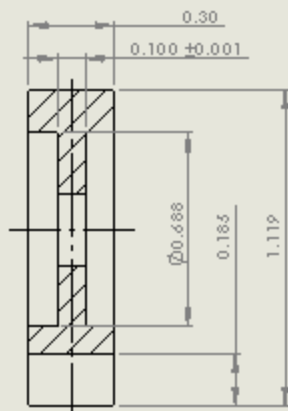
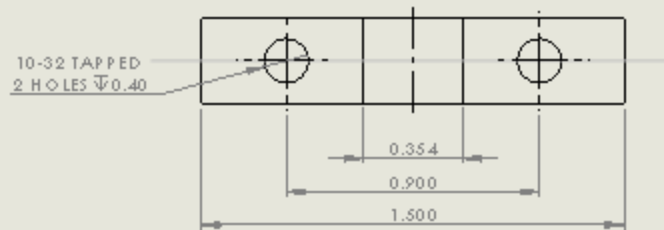


PROPERTY AND CONFIDENTIAL
THE INFORMATION CONTAINED IN THIS
DRAWING IS THE SOLE PROPERTY OF
PORTLAND STATE UNIVERSITY. ANY
REPRODUCTION IN PART OR AS A WHOLE
WITHOUT THE WRITTEN PERMISSION OF
PORTLAND STATE UNIVERSITY IS NOT
PERMITTED.

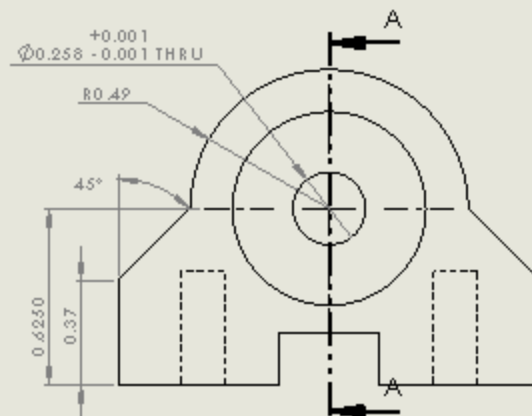
DESIGNER'S APPROVALS		DATE	DATE
DESIGN			
ENGINEER			
MECHANICAL			
WELDING			
DATA			
CONSTRUCTION			
MATERIAL	ALUMINUM		
FINISH	WETTED		
APPLICATION	DO NOT SCALE DRAWING		



EXP. DATE, NO. **A** Carriage **B.V.**
DRAWN BY **MEH** DATE **08/10/11**



SECTION A-A

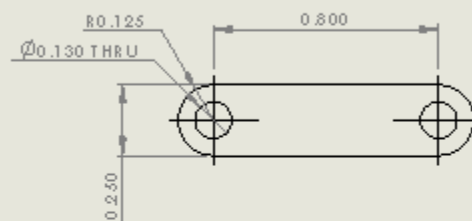
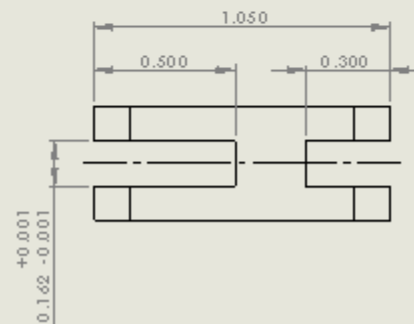
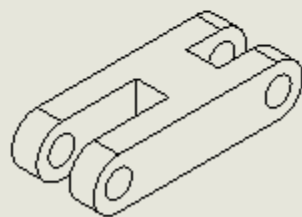


PROPRIETARY AND CONFIDENTIAL
THE INFORMATION CONTAINED IN THIS
DRAWING IS THE SOLE PROPERTY OF
PORTLAND STATE UNIVERSITY. ANY
REPRODUCTION IN PART OR AS A WHOLE
WITHOUT THE WRITTEN PERMISSION OF
PORTLAND STATE UNIVERSITY IS
NOT PERMITTED.

		DIMENSIONS ARE IN INCHES		NAME	DATE
				DRAWN	
				CHECKED	
				ENG APPR.	
				MECH APPR.	
				D.A.	
				DESIGNER	
WITNESS	USED ON	MATERIAL		DATE	
WITNESS	USED ON	MATERIAL		DATE	
APPLICATION		DO NOT SCALE DRAWING		BY	



PSAS JOURNAL
SCALE 1:1
DATE 10/1/1

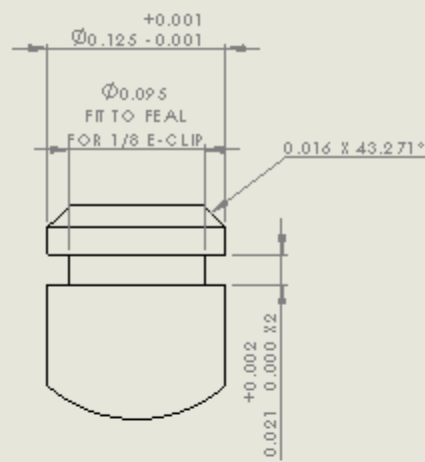


PROPERTY AND CONFIDENTIAL
THE INFORMATION CONTAINED IN THIS
DRAWING IS THE SOLE PROPERTY OF
PORTLAND STATE UNIVERSITY. ANY
REPRODUCTION IN PART OR AS A WHOLE
WITHOUT THE WRITTEN PERMISSION OF
PORTLAND STATE UNIVERSITY IS
PROHIBITED.

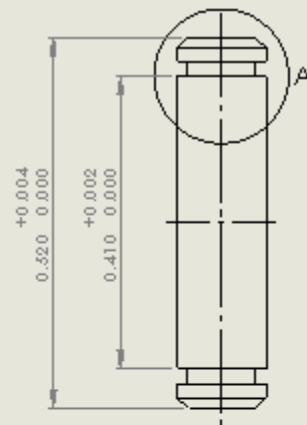
		DIMENSIONS ARE IN INCHES TOLERANCES: FRACTIONS ± .005 DECIMALS ± .001 HOLE DIA ± .001 TWO PLACE DECIMAL ± .005 THREE PLACE DECIMAL ± .001		DATE	
		MATERIAL		DESIGN	
		FINISH		CHECKED	
		TREATMENT		ENG APPR.	
		COATINGS		APP APPR.	
		OTHER		DATE	
BY ASSY	USED ON	REVISIONS			
APPLICATION		DOW NOT SCALE DRAWING			



BY: **A** DATE: **RMA_0.8-in_2** REV: **1**
SCALE: **1:1** CHECKED: **1** DESIGNED: **1**



DETAIL A
SCALE 10:1

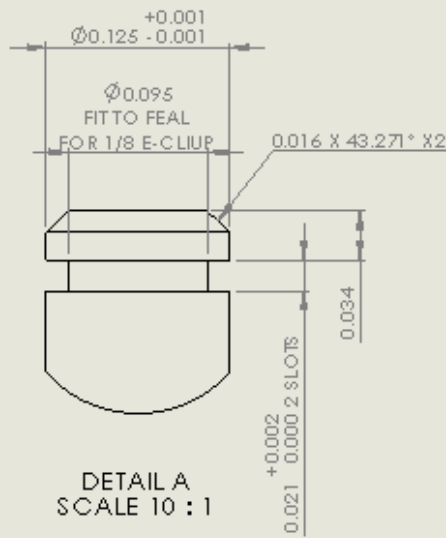


PROPRIETARY AND CONFIDENTIAL
INFORMATION CONTAINED IN THIS
DRAWING IS THE SOLE PROPERTY OF
PORT AND STATUMENTARY. ANY
REPRODUCTION IN PART OR AS A WHOLE
WITHOUT THE WRITTEN PERMISSION OF
PORT AND STATUMENTARY IS
PROHIBITED.

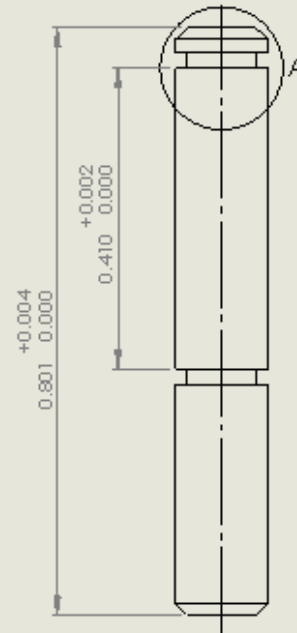
		DESIGNED BY: B. B. CHIT	DATE:	
		CHECKED BY: J. J. CHIT		
		APPROVED BY: J. J. CHIT		
		DATE:		
		REVISION:		
PROJECT NO.	1000			
APPLICATION	DO NOT SCALE DRAWING			




BY: A DOWELL
DOWELL_Fin_1
DATE: 1/1/2011



DETAIL A
SCALE 10 : 1



PROPRIETARY AND CONFIDENTIAL
 THE INFORMATION CONTAINED IN THIS
 DRAWING IS THE SOLE PROPERTY OF
 PORTLAND STATE UNIVERSITY. ANY
 REPRODUCTION IN WHOLE OR IN PART
 WITHOUT THE WRITTEN PERMISSION OF
 PORTLAND STATE UNIVERSITY IS
 PROHIBITED.

		DIMENSIONS ARE IN INCHES FRACTIONS: FRACTIONS: ANGULAR DIMENSIONS: 1/16" = 1/16" TWO PLACE DECIMALS: THREE PLACE DECIMALS:	DESIGN: REV: CHECKED: FIG APPR: WTC APPR: Q.A. COMMENTS:	DATE:		
		MATERIAL:				
		FINISH:				
NEXT ASSY:	SECTION:					
APPLICATION:	DO NOT SCALE DRAWING:					
				STW A SCALE 1:1 DWG 1 OF 1	DWG NO: Dowell_Pin_2 DWG 1 OF 1	REV: